An Investigation of the Photoredox Radical Smiles Rearrangement

A thesis submitted to The University of Manchester for the degree of Master of Philosophy (MPhil) in the Faculty of Science and Engineering

2021

Weng Ieong

School of Chemistry

Contents

Word Count: 14489

List of Schemes

List of Tables

Abbreviations

A	acceptor molecule
Ac	acetate
ACCN	1,1'-azobis(cyclohexanecarbonitrile)
AIBN	azobisisobutyronitrile
Ar	aryl
ART	aryl radical transfer
BDE	bond dissociation energy
BET	back electron transfer
bpy	2,2'-bipyridine
Bu	butyl
cat	catalyst
conc.	concentration
D	donor molecule
DABCO	1,4-diazabicyclo[2.2.2]octane
DBU	1,8-diazabicyclo(5.4.0)undec-7-ene
DCC	*N,N*'-dicyclohexylcarbodiimide
DCE	dichloroethane
DIPEA	*N,N*-diisopropylethylamine
DMA	dimethylacetamide
DMAP	4-dimethylaminopyridine
DMF	dimethylformamide
DMSO	dimethyl sulfoxide
dtbbpy	4,4'-di-tert-butyl-2,2'-dipyridyl
e.g.	for example
EA	ethyl acetate
EDA	electron-donor-acceptor
EDC.HCl	1-ethyl-3-(3-dimethylaminopropyl)carbodiimide hydrochloride
EnT	energy transfer
equiv	equivalents
ESI	electrospray ionization

Et	ethyl
EWG	electron-withdrawing group
Fc	ferrocene
g	gram
h	hour
HAT	hydrogen atom transfer
HetAr	heteroaryl
HEX	hexane
HOMO	highest occupied molecular orbital
HRMS	high-resolution spectroscopy
hv	light
Hz	Hertz
kcal	kilocalories
L	litre
LUMO	lowest occupied molecular orbital
M	molar concentration
Me	methyl
Mes-Acr	mesityl acridinium
MLCT	metal-ligand charge transfer
mol	mole
n.r.	no reaction
NMR	nuclear magnetic resonance
NPhth	phthalimide
^{o}C	degree Celsius
OQC	oxidative quenching cycle
OTf	triflate
PC	photocatalyst
ppm	parts per million
ppy	2-phenylpyridine
Pr	propyl
quant.	quantitative

RQC	reductive quenching cycle
s	second
s.m.	starting material
SCE	saturated calomel electrode
SET	single electron transfer
S_NAr	nucleophilic aromatic substitution
SOMO	singly occupied molecular orbital
TBAF	tetra-*n*-butylammonium fluoride
TBS	*tert*-butyldimethylsilyl
THF	tetrahydrofuran
TLC	thin layer chromatography
TMEDA	tetramethylethylenediamine
TMG	1,1,3,3-tetramethylguanidine
TTMSS	tris(trimethylsilyl)silane
UV	ultraviolet
V	volt
W	watt
λ	wavelength

Abstract

Photoredox catalysis is the core interest in our study of radical Smiles rearrangements across this work. The radical Smiles rearrangement is a robust reaction used for sp^3-sp^2 and sp^2-sp^2 coupling and we aimed to use visible light energy to operate this transformation, using cheap and abundant carboxylic acid derivatives as starting materials. Multiple ways of radical generation were used when investigating the radical Smiles rearrangement on sulfonates and sulfonamides.

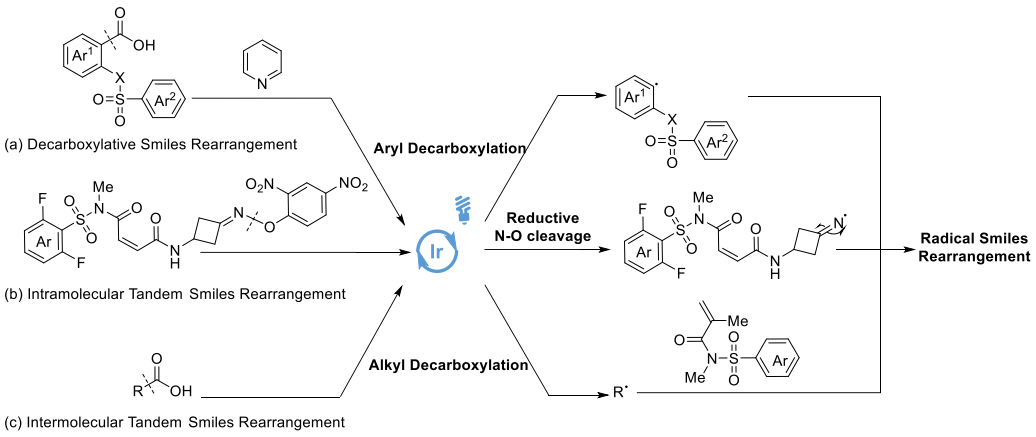

In the visible-light mediated intramolecular aryl-aryl coupling of aryl sulfonamido-benzoic acids (a), pyridine was identified to be an effective base in deprotonating the benzoic acid in one of the aryl sulfonylamidobenzoic acid substrates. This facilitated the decarboxylation of the in-situ generated benzoate-hypobromite intermediate, leading to aryl radical generation. Rather than the aryl-aryl Smiles coupling, the generated aryl radical preferred two other quenching pathways: either hydrogen abstraction or pyridine coupling.

Distant cyano-alkyl radical generation from cyclobutyloxime cleavage (b) was used in the investigation of the intramolecular tandem Smiles rearrangement while alkyl decarboxylative generation of radicals from alkyl *N*-hydroxyphthalimide (c) was used in the study of the intermolecular approach on a sulfonyl methacrylamide. Surprisingly, the alkene functional group in both cases was found to be unstable in our mild photo conditions. The maleimide-like alkene was found to be sensitive to trialkylamine base while the alkene in the methacrylamide was found to interrupt the designed alkyl decarboxylative photocatalytic system.

Declaration

No portion of the work referred to in the thesis has been submitted in support of an application for another degree or qualification of this or any other university or other institute of learning.

Copyright Statement

Acknowledgement

I would like to express my greatest gratitude to my research supervisor Prof. Michael F. Greaney for his invaluable advice and guidance throughout my research. I would also like to thank my co-supervisor Prof. David J. Procter for his support on my MPhil thesis. I would particularly like to thank all the Greaney group members for the insights and enlightenment to my MPhil research. Finally, I would like to give thanks to my dear family and friends for all the encouragement and care.

Chapter 1 Background

1.1 Principle of Photoredox Catalysis

Photoredox catalyst was first demonstrated within organic synthesis in the 1980s. Using visible light in organic synthesis is desirable due to its renewable and environmentally friendly nature. The maximum absorption range of most organic molecules falls within the UV region so they are unable to be directly excited by visible light. However, photocatalysts, which have significant absorption in the visible-light range,[1] are capable of transferring visible-light energy to organic molecules through electron transfer events, making them a powerful tool in visible-light mediated reactions.

Oxidative Quenching and Reductive Quenching

In photoredox catalysis, the photocatalyst can interact with the organic molecule through two general pathways, the oxidative quenching cycle (OQC) and the reductive quenching cycle (RQC). In a photoreaction, the ground-state electrons of the photocatalyst, upon light irradiation, are excited into the singlet excited state ($d\pi \rightarrow \pi^*$), which may undergo a spin-forbidden transition through intersystem crossing into the triplet excited state. The excited electrons will have a lifetime in the order of μs, which is long enough for electron transfer events that occur in the order of ns or ps to take place.[2]

In the oxidative quenching cycle, the excited triplet state photocatalyst species is oxidized through a single electron transfer (SET) process by an acceptor molecule, generating $\mathbf{PC}^{+\cdot}$ and $\mathbf{A}^{-\cdot}$ *(Scheme 1a)*. In this process, the electron in the higher **SOMO** serves as the reductant during the SET event. Subsequently, a donor molecule will then be responsible for donating an electron to the $\mathbf{PC}^{+\cdot}$ species through a SET event to regenerate the **PC**. Meanwhile in the reductive quenching cycle, the excited photocatalyst is reduced by a donor molecule to $\mathbf{PC}^{-\cdot}$ and generating $\mathbf{D}^{+\cdot}$. In this

process, the hole in the lower **SOMO** serves as the $1e^-$ oxidant. The reduced photocatalyst $\mathbf{PC}^{-\cdot}$ is subsequently oxidized by an acceptor molecule **A** to restore **PC**.

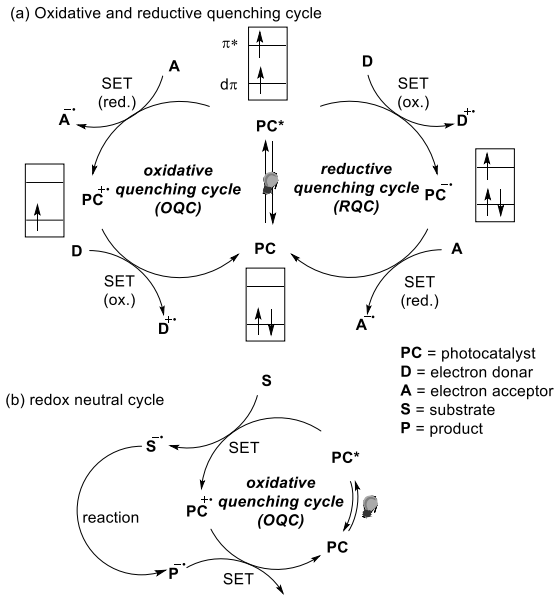

Scheme 1 Principle of photoredox catalysis (Reproduced from [1])

The donors and acceptors in the mechanism are the actual substrate in the organic transformation, the photoredox catalyst allowing for the mild, selective generation of radicals which can go on to undertake a plethora of subsequent transformations. It is worth noting that the acceptor/ donor molecules that interact with the photocatalyst do not have to belong to the same substrate, but when they do, the catalytic cycle is considered to be redox neutral *(Scheme 1b)*. Otherwise, a sacrificial reductant or oxidant must be present to act as the second acceptor or donor in turning over the photocatalyst.

Choice of photocatalyst

The redox potentials of transition-metal photoredox catalysts are determined by the nature of the metal centre, the charge of the metal and the ligand, and the electrostatic interaction between the metal centre and the chelating ligands.[2] The redox potentials of photocatalysts are typically enhanced upon their photoexcitation.[3] For instance, during the reduction process of the substrate in the OQC, the **HOMO** energy level is a rough estimation of the reducing power of the photocatalyst. The

reducing power of the photo-excited catalyst however is further enhanced by the energy gap between the **HOMO** at the ground state and the higher **SOMO** at the excited triplet state, as depicted by the dashed ellipse on *Scheme 2*.[1] Vice versa during the oxidation of the substrate in RQC, the oxidizing power of the photocatalyst in its excited state is enhanced by the **LUMO** and the lower **SOMO** at the excited triplet state, as shown by the solid ellipse on *Scheme 2*. The difference upon the enhancement is comparable to the **HOMO/ LUMO** gap estimated from the visible-light absorption.

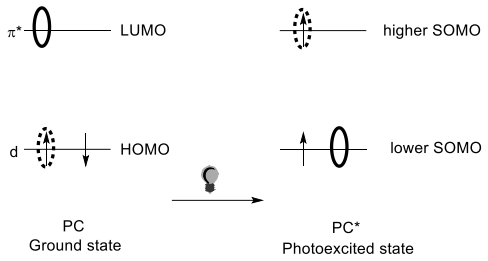

Scheme 2 Oxidizing and reducing power enhancement of photocatalyst after photoexcitation (Reproduced from [1])

Some examples of common transition metal photocatalysts are shown in *Table 1*. In the design of a photocatalytic system, proper selection of the photocatalyst is crucial for driving the organic transformation. For instance, the reductive transformation of the substrate in the OQC, a catalyst with a $^{*}\mathbf{PC}^{n+}/\ \mathbf{PC}^{(n-1)+}$ value more negative than that of the substrate is desirable thermodynamically. Organic photosensitizers have had more attention drawn towards their photocatalytic applications due to their ease of preparation and cheaper price compared to metal-based catalysts. Popular examples include methylene blue, eosin Y, rose bengal and acridinium salts. Among the organophotocatalysts, mesityl acridinium fluoride is well known for its strong oxidizing power.

Table 1 Redox potential of commonly used photocatalysts. (Reproduced from [1])

Catalyst	λ_{max} (nm)	$*PC^{n+}/ PC^{(n-1)+}$ [a]	$PC^{(n+1)+}/ *PC^{n+}$ [a]
$[Ru(bpy)_3]^{2+}$	452	0.43	-1.24
$Ir(ppy)_3$	375	-0.10	-2.14
$[Ir(dtbbpy)(ppy)_2]^+$	400	0.5	-1.37
$[Ir(dF(CF_3)ppy)_2(dtbbpy)]^+$	380	0.48	-1.62
$[Ir(dF(CF_3)ppy)_2(bpy)]^+$	412, 379	0.91	-1.41
Methylene blue	664	1.34	/
Eosin Y	539	0.80	-1.98
Rose bengal	548	0.61	-1.06
$MesAcr^+ClO_4^-$	430	1.65	/

a. Potential in V (vs Fc/ Fc*)

1.2 Smiles Rearrangement

Polar Smiles Rearrangement

The Smiles rearrangement is an intramolecular S_NAr reaction of an activated arene, preferentially with an electron-withdrawing group substituted at the *ortho*- or *para*-position.[4] The rearrangement begins with the nucleophilic attack of arene **1.1** by a strong nucleophile Y (e.g. thiol, alcohol, amine), forming a C-Y bond, and generating a Meisenheimer complex where X is the nucleofuge that is capable of carrying the negative charge as a leaving group (e.g. sulfone, sulfide, ether) *(Scheme 3)*. Collapse of the Meisenheimer intermediate and breaking of the C-X bond then leads to the migration of the aryl group affording **1.2**.

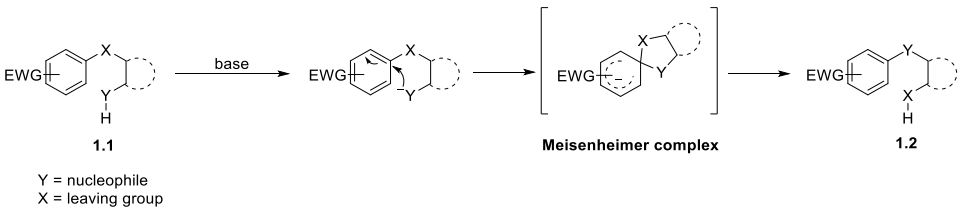

Scheme 3 Mechanism of the Polar Smiles rearrangement

The reaction was initially reported by Henriques[5] in 1894 followed by Hinsberg[6] on naphthosulfones. More studies on the nature of the Smiles reaction were published[7]

in the 1930s when Truce *et al.* outlined a comprehensive description on the conditions that facilitate the migratory system. [8] They developed the carbanion Smiles reaction using an organolithium base to perform the aryl migration on sulfone **1.3** with an unactivated arene, where a new C-C bond was formed after the aryl migration affording **1.5** *(Scheme 4)*. The Smiles rearrangement was completed with treatment of acid, releasing the SO_2 to give Smiles product **1.6**.[9] This type of reaction was then regarded as the Truce-Smiles rearrangement.

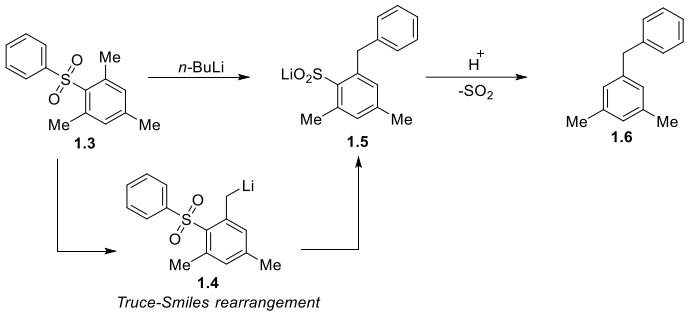

Scheme 4 Truce-Smiles rearrangement of mesityl sulfone

1.2.1 Radical Smiles Rearrangement

Radical Smiles chemistry was unravelled by Speckamp after numerous reports of ionic polar Smiles rearrangements in 1977.[10] Speckamp reported the 1,4-*p*-tolyl migration on a simple piperidine and applied the method to a functionally substituted piperidine derivative, initiated by a methylene radical generated from carbon-halogen cleavage using stoichiometric tin hydride. The radical Smiles rearrangement is initiated by a free radical Y attack on the *ipso*-position of the aryl sulfonate or sulfonamide forming the Meisenheimer intermediate, followed by extrusion of SO_2 and hydrogen abstraction to complete the aryl migration *(Scheme 5)*. Later, Motherwell demonstrated the application of the radical Smiles rearrangement in the synthesis of biaryls,[11] which aroused more attention towards the radical Smiles rearrangement.

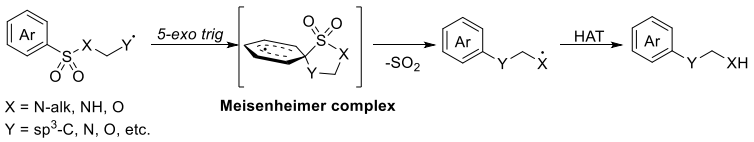

Scheme 5 Mechanism of radical Smiles rearrangement.

Compared to the polar-Smiles reactions, the radical approach enables the use of milder conditions to complete the aryl migration. Many of these examples have exploited the light-induced generation of radicals to perform the Smiles rearrangement. A prominent example was demonstrated by Stephenson *et al.* during the synthesis of an opioid-receptor like ORL-1 antagonist *(Scheme 6)*.[12] A thiophene group was migrated to a difluoro unit through a radical Smiles rearrangement on a thiophene sulfonate. Later, the preparation of the thiophene starting material was scaled up to 100 g using flow chemistry techniques.[13]

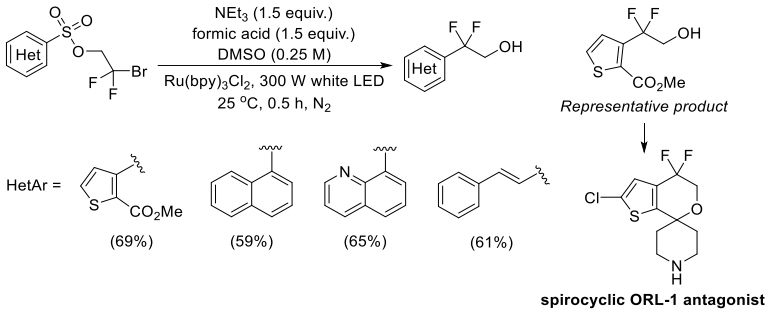

Scheme 6 Selected example for Smiles rearrangement in synthesis of spirocyclic ORL-1 antagonist

Apart from the synthesis of small molecules, radical Smiles rearrangements have been applied to the total synthesis of larger drug molecules. Banwell *et al.* utilized the radical Smiles rearrangement as a key step in the seven-step synthesis of the D-ring isomer of galanthamine *(Scheme 7)*.[14] The alkyl radical formed from the ethyl-bromo bearing tertiary amine underwent a sp^3-sp^2 Smiles through a 5-exo trig pathway, forming an α-amino alkyl radical that could then add onto the cyclohexene in an 8-endo trig cyclization. Completion of the reaction by rearomatization followed by deprotection steps gave the galanthamine isomers.

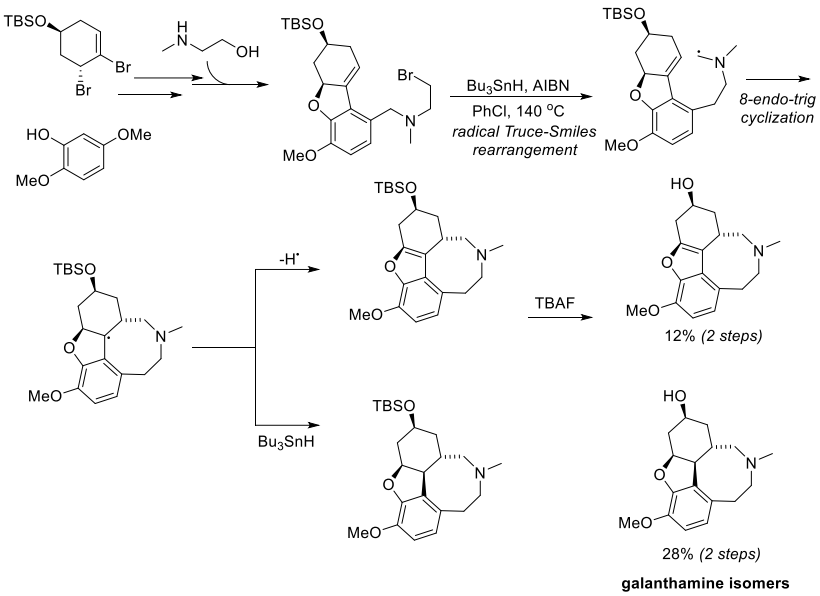

Scheme 7 Radical Smiles example in synthesis of galanthamine isomers

Chapter 2 Introduction

2.1 Alkyl and aryl decarboxylation

Alkyl radical generation

Alkyl carboxylic acids are versatile components in organic synthesis. Aside from being a robust coupling partners in ester synthesis, amide synthesis, and multicoupling reactions (e.g. Ugi, Passerini),[15] functionalization via the decarboxylative generation of alkyl radicals has further broadened its applicability. The precursors, alkyl *N*-hydroxyphthalimide esters, can be easily prepared by coupling *N*-hydroxyphthalimide with a carboxylic acid and these redox-active esters are used for generating primary, secondary, and tertiary alkyl radicals under mild conditions, such as with a photocatalyst *(Scheme 8)*.

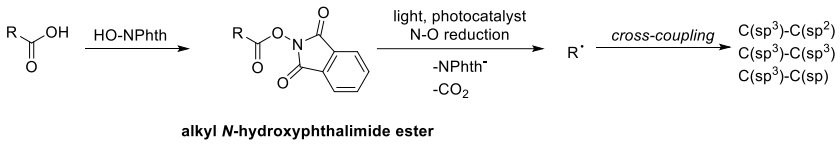

Scheme 8 Decarboxylative coupling of alkyl N-hydroxyphthalimide ester

During decarboxylation, the oxidized photocatalyst formed upon the *N*-hydroxyphthalimide reduction is usually regenerated via three catalytic pathways[16]: *i)* employing an additional reductant, *ii)* using a low-valent metal intermediate as a reductant in dual catalysis, *iii)* utilizing the radical intermediates as reductants. Among the three pathways, we are most interested in the first approach during the investigation of the Smiles rearrangement. Various types of C-C bond formation have been demonstrated using this strategy *(Scheme 9)*.[16-17] With the pioneering examples presented by Okada and Ka,[17a] Fu and Yang, [17c] König,[17b] Maestro and Alemán, [17f] Witte and Minnaard,[17k] Cong, [17d] Mariano and Wang, [17e] on the Giese type reaction of adding the alkyl radical to the Michael acceptor, we hope to take advantage of these examples to investigate our tandem radical Smiles rearrangement *(See Section 2.3)*.

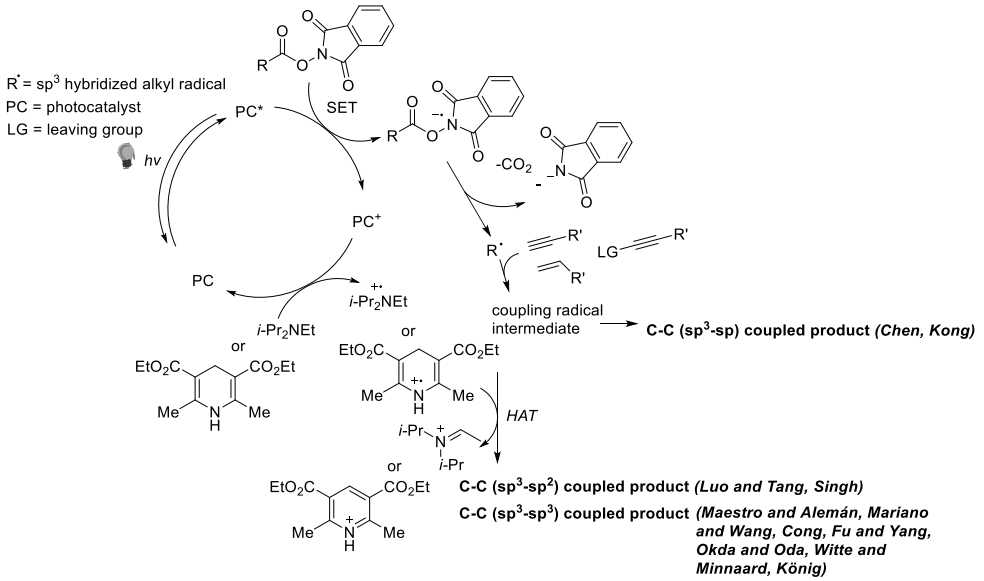

Scheme 9 General mechanism of photocatalysed decarboxylative coupling of alkyl N-hydroxyphthalimide ester using additional reductant

Aryl radical generation

Aryl radicals are also versatile intermediates in organic synthesis. Since their first use, as demonstrated by the Meerwein reaction,[18] these radicals have become important intermediates in functional group conversions and C-H bond functionalizations *(Scheme 10)*.[19]

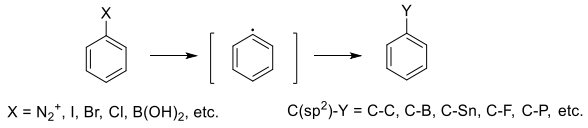

Scheme 10 Traditional generation and transformation of aryl radicals

Common aryl radical precursors include diazonium salts, halides, triflates, boronic acids, hypervalent iodines, and sulfonium salts *(Scheme 10)*.[20] However, the unstable nature or complicated preparation processes of many of these precursors have hindered their applicability. On the other hand, stable, cheap, and readily available carboxylic acids are extremely attractive as aryl radical precursors in organic synthesis. Applications of carboxylic acids compared to other precursors have been explored less

extensively due to the difficulty in generating aryl radicals,[21] particularly under mild conditions.[22]

Despite the versatility of decarboxylating alkyl carboxylic derivatives using photocatalysts,[16-17] direct aryl radical formation from benzoic acids remains difficult in organic synthesis. After deprotonation of the benzoic acid, the oxidation of the resulting benzoate has to overcome the back electron transfer process (BET) to generate a benzoate radical *(Scheme 11)*. As well as this, other competitive pathways such as intermolecular hydrogen atom abstraction ($k = 1.2 \times 10^7$ M^{-1} s^{-1}) or addition to arenes ($k = 2.2 \times 10^8$ M^{-1} s^{-1}) are also significant due to the relatively sluggish kinetics in the desired aryl decarboxylation ($k = 1.4 \times 10^6$ s^{-1}).[21]

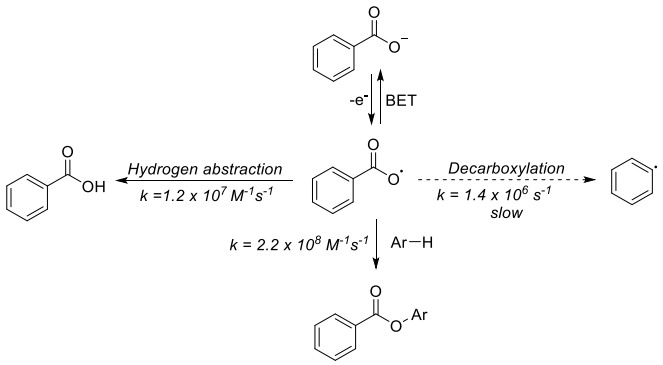

Scheme 11 Competitive reactions for benzoyl radical decarboxylation

In early decarboxylative reactions, harsh conditions such as high temperatures were often required to access direct aryl decarboxylations. In 2012, Greaney *et al.* reported oxidative aryl decarboxylation using a silver (II) catalyst *(Scheme 12)*.[22] Upon oxidation by the silver (II) catalyst, decarboxylation, driven by high thermal conditions (100 °C), could generate an aryl radical which was subsequently terminated by a HAT process with the solvent. This method allows decarboxylation to proceed without the presence of *ortho*-substituents. However, by derivatising the benzoic acid into *N*-hydroxyphthalimide esters or oxime esters, milder conditions can be employed to access aryl radicals using visible-light energy. In 2017, Glorius *et al*. discovered a visible-light mediated decarboxylative coupling of *N*-hydroxyphthalimide esters with B-pin upon reduction of the photoexcited phthalimide acceptor by pyridine-diboronate ester Lewis adducts.[23] Later, the same group reported the photosensitized homolytic

N-O cleavage and decarboxylative fragmentation of oxime esters to give aryl or alkyl radicals in a concerted pathway, which were then trapped to form carbon-heteroatom or carbon-carbon bonds.[24]

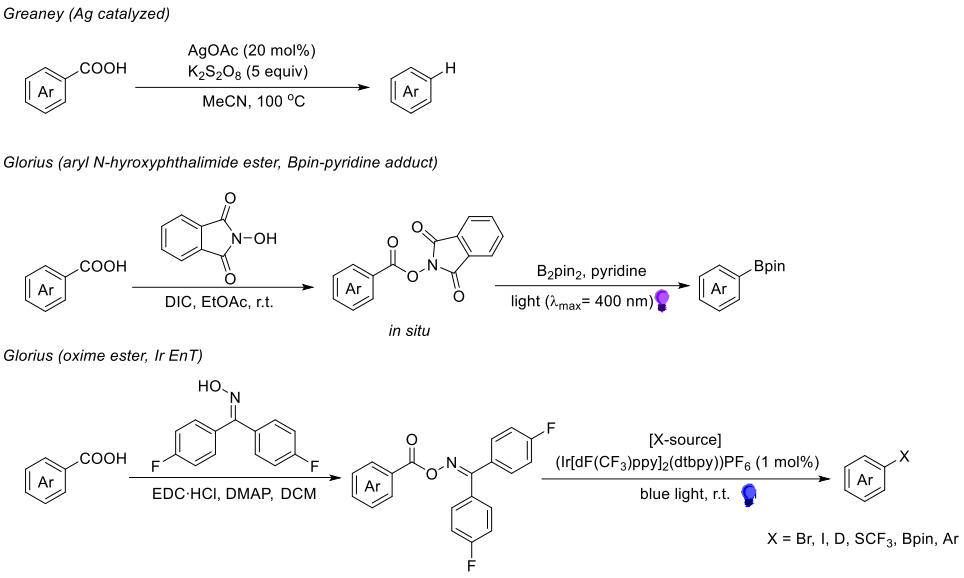

Scheme 12 Aryl decarboxylative coupling of benzoic acid and its derivatives

Recently, Ritter and Macmillan separately reported the visible-light induced MLCT of copper (II) carboxylates to trigger Cu-O bond homolysis followed by aryl decarboxylation to give an aryl radical *(Scheme 13)*.[25] This radical was subsequently trapped either by a stoichiometric copper (II) complex, giving a hypervalent copper (III) intermediate which was used to access C(sp^2)- F coupling, or it was trapped by another halo radical to form a C-X bond, respectively.

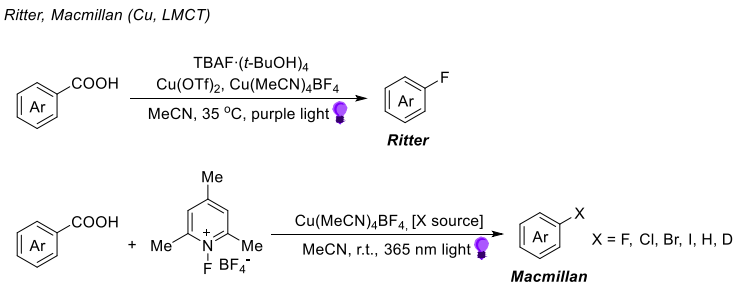

Scheme 13 Copper-catalysed MLCT-decarboxylative coupling of benzoic acids

Most of aryl decarboxylation methods are only amenable towards carbon-heteroatom bond formation. In recent work,[26] Glorius demonstrated trapping of the aryl radicals with arenes and heteroarenes following a mild aryl decarboxylation within a reductive quenching cycle *(Scheme 14)*. After deprotonation of the benzoic acid, the benzoate anion was oxidized by the photoexcited iridium catalyst. The benzoate radical then reacts with the bromine source, in their case, diethyl 2-bromo-2-methylmalonate, to give a hypobromite intermediate. They showed that reduction of the aryl hypobromite intermediate could facilitate concerted decarboxylation to generate an aryl radical that can be trapped by arenes and heteroarenes to form a $C(sp^2)$-$C(sp^2)$ bond. The generation of aryl radical from benzoic acid gives hope that the direct decarboxylative aryl Smiles rearrangement would be successful.

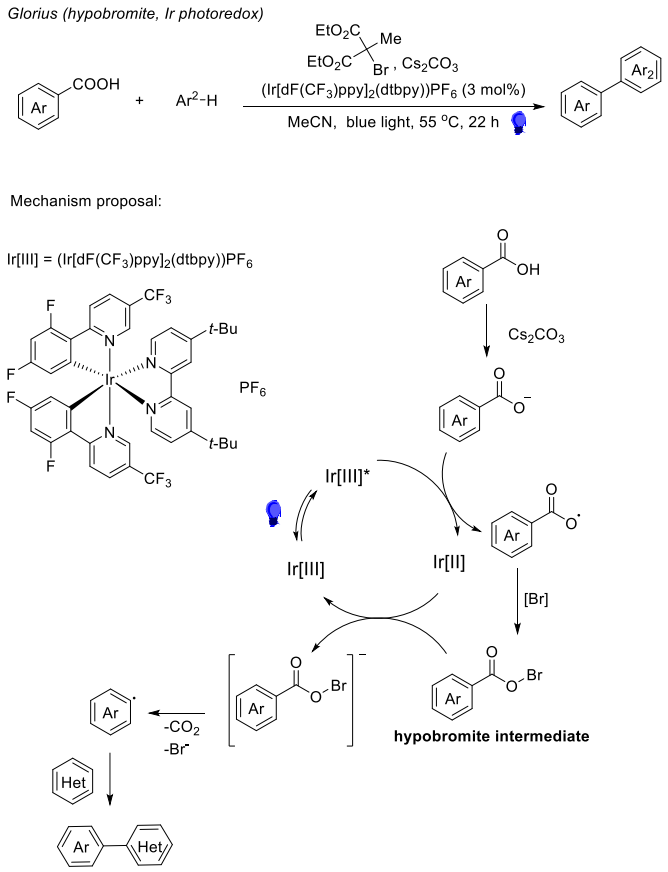

Scheme 14 Mechanism of visible-light mediated aryl radical generation from benzoic acid via formation of hypobromite intermediate

2.2 Aryl-aryl radical Smiles coupling

Many of the Csp^2- Csp^2 coupled radical Truce-Smiles rearrangements involve the use of alkyne starting materials to give vinylic products.[27] On the other hand, aryl-aryl C-C coupling in the radical Smiles rearrangement is less well-explored. The group of Motherwell have greatly contributed to our understanding of aryl-aryl ipso-coupling via the Smiles rearrangement[11a] and have recently discussed the limitations and factors that that lead to the preferential 1,5-*ipso*-substitution over 1,6-addition upon the aryl radical formation *(Scheme 15)*.[28] The 1,5-*ipso*-substitution can be tuned in favour over the 1,6-cyclization by controlling the stoichiometry, the concentration, the rate of addition of *n*-Bu_3SnH, solvent system, and reaction temperature. It was found that both electron-withdrawing and electron-donating *ortho*-substituents on the acceptor ring are good 1,5-*ipso* directors. Among the three linkers they have tested—namely sulfonamide, carbonate, and sulfonate linkers, substrates with a sulfonamide linker gave the greatest ratio of 1,5-*ipso*-substitution products. This is most likely to be ascribed to the faster extrusion of SO_2 from the adjacent N compared to the O atom.

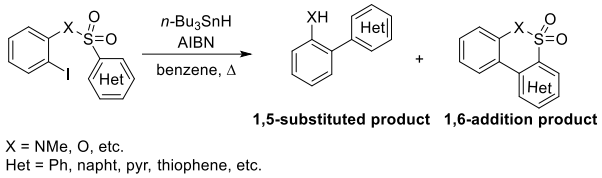

Scheme 15 Aryl-aryl coupling using iodoarylsulfonate or sulfonamide

Recently, Han, Lambert, and Hertweck developed methods for radical aryl-aryl coupling using iodoarenes or sulfonamide linked precursors. Han *et al.* reported the synthesis of a series of biaryl amines *(Scheme 16)*.[29] Using aryl sulfonamide substituted diaryliodinium salts, an EDA complex was formed by its association with triethylamine, which upon heat activation could generate aryl radicals. These radicals proceeded through the radical Truce-Smiles rearrangement as the major pathway to provide valuable biaryl amine products.

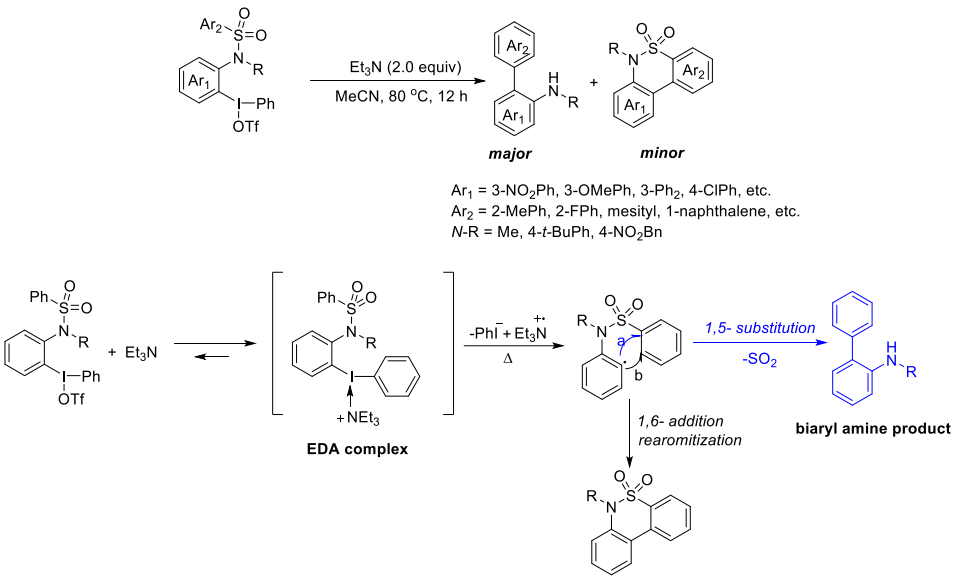

Scheme 16 Biaryl synthesis from diaryliodinium salts

Lambert *et al*. demonstrated the photoredox-catalysed aryl radical transfer (ART) using iodo-arene precursor and $Ir(dtbbpy)(ppy)_2PF_6$ *(Scheme 17)*.[30] The iodoarene was reduced by the Ir(III) catalyst to generate an aryl radical, which triggered the ART followed by release of SO_2 to afford the biaryl product.

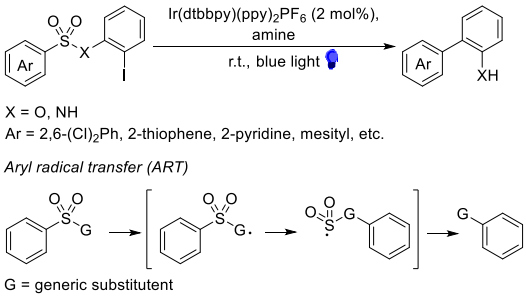

Scheme 17 Photoredox catalysed biaryl synthesis from iodoarylsulfonamide using aryl radical transfer (ART)

Hertweck *et al*. discovered that a sulfonamide linker could direct the fusion of two aryl groups *(Scheme 18)*.[31] It was proposed that UV irradiation could lead to homolytic fission of the linker, followed by a Smiles-like coupling of the two aryl radicals to give the biaryl products. Interestingly, the linker was split into three parts and lost as SO_2, NH_3, and formaldehyde in the coupling reaction. Using this so-called photoslicing

approach, they were able to synthesize a range of valuable precursors for drug synthesis.

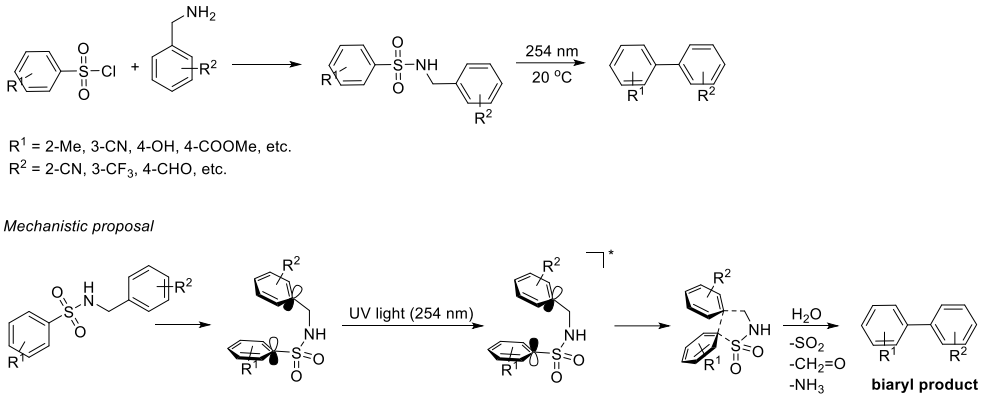

Scheme 18 UV initiated aryl-aryl coupling via cleavable sulfonamide linker

Louis *et al.* developed a dimeric gold system to access carbon-centered radical intermediates from unactivated alkyl (E_{red}= -1.90 to -2.50 V vs SCE) and aryl bromides (E_{red} = -2.05 to -2.57 V vs SCE) under either mild UV irradiation or natural sunlight which was followed by either inter or intramolecular addition.[32] A Smiles rearrangement was observed in one of their substrates *(Scheme 19)*. The aryl radical was produced from an aryl bromo-sulfonamide which then performed an intramolecular *ipso*-substitution to afford biarylamine as the major product (63:37).

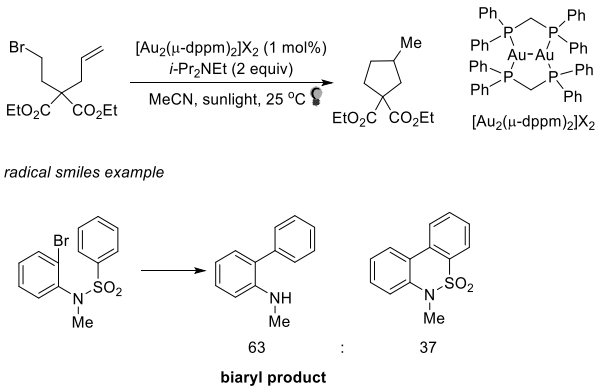

Scheme 19 Dimeric gold catalysed aryl-aryl coupling

Though effective, these methods involve the use of less readily available aryl halides derivatives as precursors to aryl radical generation. We aimed to explore the possibility

of utilizing naturally abundant aryl carboxylic acid derivatives to perform aryl-aryl coupling via radical Smiles rearrangement.

2.3 Tandem radical Smiles rearrangement

In the tandem radical Smiles rearrangement, after the generation of the primary radical, a secondary radical is generated through a radical cascade, which is responsible for performing the radical Smiles rearrangement. The secondary radical generation is most often achieved by adding the first radical onto a Michael-acceptor. Sapi *et al.* illustrated this concept on the first domino radical Smiles cyclisation rearrangement in 2012 *(Scheme 20)*.[33] The alkyl radical was generated from the reduction of the aryl halide, followed by a Giese-type reaction towards an internal electron-deficient alkene, then a successive Smiles rearrangement which afforded 3-substituted indolin-2-one products.

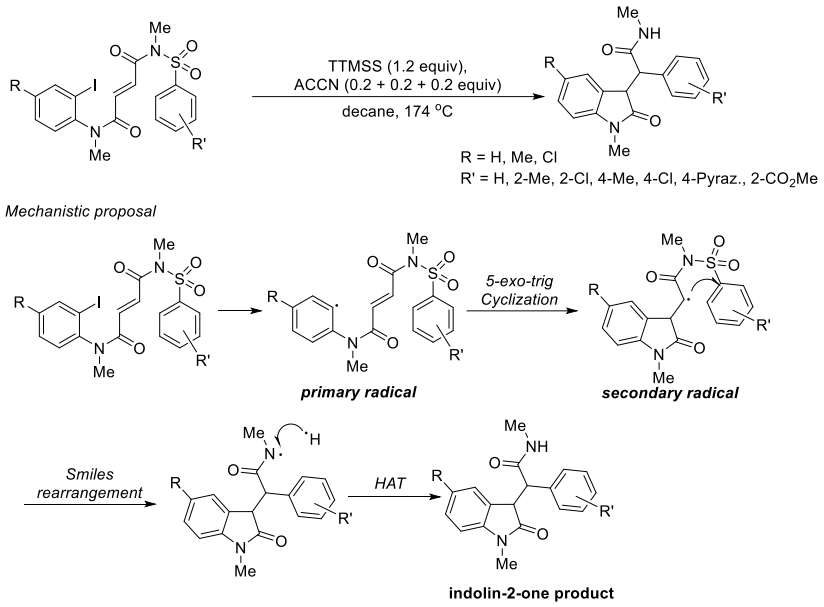

Scheme 20 Tandem radical Smiles cyclization example of aryl halides

In 2021, Liu *et al*. studied the aminoarylation of alkenes via the N-centered radical cyclization domino Smiles process to obtain an arylethylamine containing 1,4,5,6-tetrahydropyridazines *(Scheme 21)*. [34] The hydrazone was deprotonated under basic conditions to give the corresponding anion, which was later oxidized by photoexcited $*[Ru(bpy)_3]^{2+}$ to generate the N-centered radical. This electrophilic radical underwent a

6-*exo-trig* cyclization onto the alkene forming an alkyl radical that could trigger aryl migration through a radical Smiles mechanism to afford 1,4,5,6-tetrahydropyridazines as the final product.

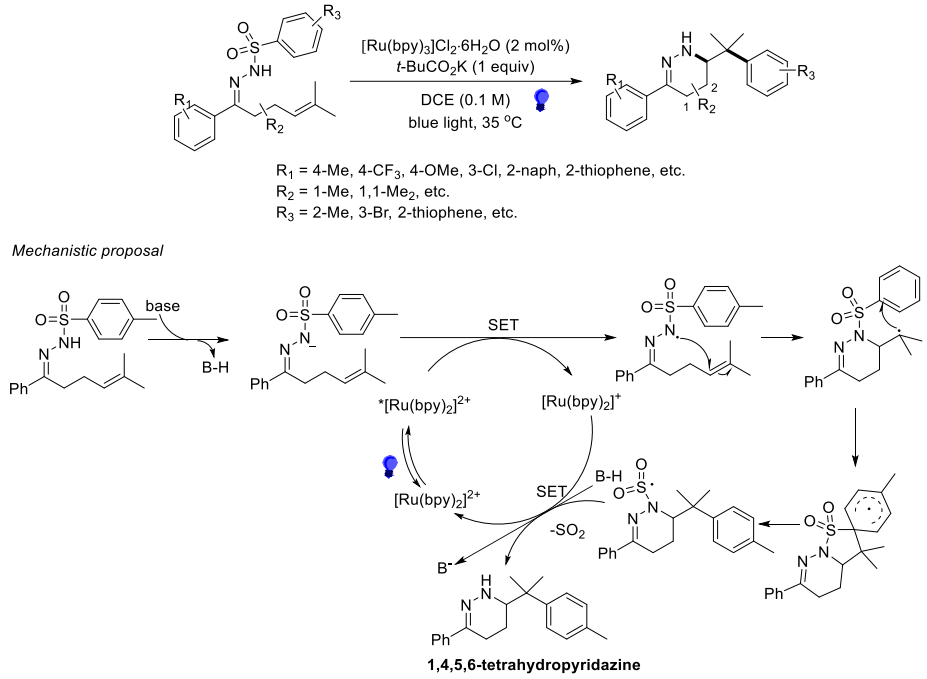

Scheme 21 Tandem radical Smiles cyclization example of hydrazones.

Nevado *et al*.[35] disclosed various examples of this reaction in an intermolecular fashion utilizing the sulfonyl acrylamide substrate. Later, Zhang,[36] Hu,[37] Zhou,[38] Kuang,[39] Pan,[40] and Greaney[41] have shown the versatility of the arylamide substrate and its analogous using different radicals and radical generation methods *(Scheme 22)*.

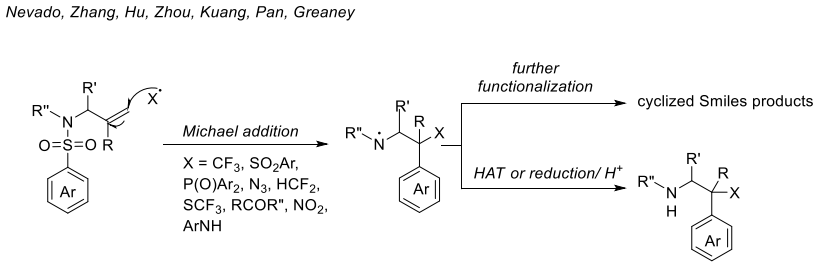

Scheme 22 Radical Smiles example utilizing sulfonyl acrylamide substrate

Surprisingly, visible-light mediated functionalization of a sulfonyl acrylamide was relatively rare and recently Greaney *et al*. discovered a photo-mediated radical Truce-

Smiles reaction on the related *N*-allyl sulfonamide substrate (*Scheme 23)*.[41] The difunctionalization of the alkene began with the reduction of the photoexcited ethyl bromodifluoroacetate-trialkylamine EDA complex to give an alkyl radical which participated in the same Michael-addition type cascade as the aforementioned acrylamides.[35] The reaction afforded valuable β-*gem*-difluoro arylethylamide structures.

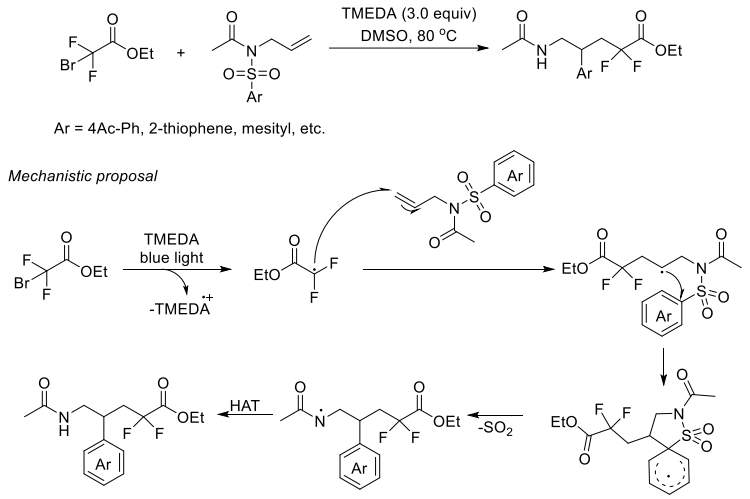

Scheme 23 Visible-light mediated radical Smiles reaction on N-allyl sulfonamide substrates

Zhang *et al*. used an unusual layered BiOBr nanosheet semiconductor in the trifluoromethyl radical generation for their functionalization of sulfonyl methacrylamides *(Scheme 24)*.[36] The key photochemical step involved the promotion of electrons from the valence band to the conduction band upon light absorption of BiOBr followed by transfer of the electron to CF_3SO_2Cl. The reduced CF_3SO_2Cl then collapsed to expel SO_2 and chloride anion, forming CF_3 radical.

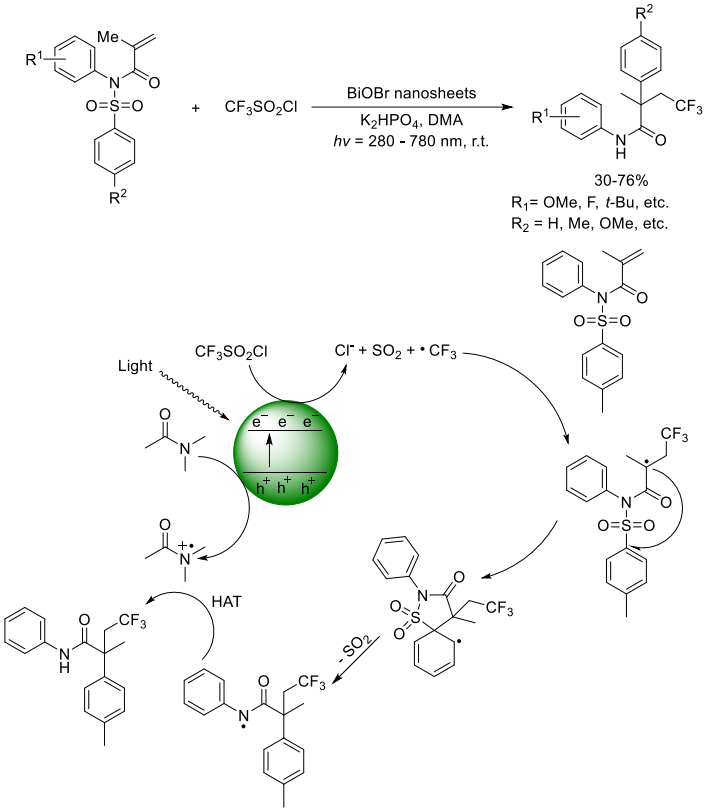

Scheme 24 BiOBr nanosheet catalysed radical Smiles rearrangement on sulfonyl methacrylamides

Recently, Greaney and Whalley[42] are reporting on Nevado's work,[43] an asymmetric radical Smiles rearrangement on N-arylsulfinyl acrylamides to give an acyclic amide product with an α-quaternary centre *(Scheme 25)*. The configuration of the products could be controlled by changing the chirality of the auxiliary sulfoxide group, and an extremely broad scope of 50 examples were shown by adding a range of different radicals (SO_2Ar, CF_3, CR_3, …) to the vinyl moiety. A photochemically generated radical was added to the double bond to give a tertiary alkyl radical that reacted enantioselectivly via a spirocyclic transition state to give SO-centered radical intermediate. This sulfur radical was quenched by Ir(IV) and water to give the desired product whilst turning over the Ir catalyst.

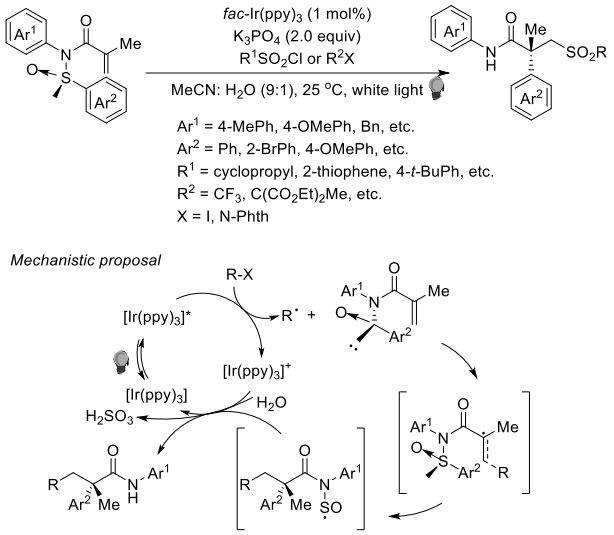

Scheme 25 Photoredox radical Smiles rearrangement on sulfinyl methacrylamide

Inspired by the intramolecular example using aryl halides from Sapi[33] and the intermolecular example using acrylamides from Nevado,[35, 43] we hope to use photoredox catalysis to investigate both the inter- and intramolecular tandem Smiles reactions.

2.4 Radical Smiles rearrangement on carboxylic acid derivatives

Alkyl decarboxylative Smiles rearrangement

With the aid of a photocatalyst, an alkyl radical can be generated from easily prepared carboxylic acid derivatives under mild conditions to then undergo a radical Smiles rearrangement *(see Section 2.1 on page 22)*.[16] Reiser *et al*. reported the decarboxylative radical Smiles rearrangement of ω-aryl-*N*-(acyloxy)phthalimides in the synthesis of dihydroisoquinolinones, benzoazepinones, and phenylethylamine derivatives from commercially available amino acids, benzaldehydes, or benzoic acids *(Scheme 26)*.[44] This method was applied in the synthesis of enantiopure D-amphetamine and capsazepinoid bronchodilators precursors, both of which belong to important biological substance classes. Interestingly, despite the use of a redox active phthalimide ester, the reaction was initiated via energy transfer from the Ir (III) catalyst to the protonated substrate, which triggered intramolecular electron transfer (IET) followed by decarboxylation to form the alkyl radical. Different cyclized products

were observed, dependent on the chain length of the alkyl radical from the ω-aryl-*N*-(acyloxy)phthalimides and the electronic property of the aryl ring.

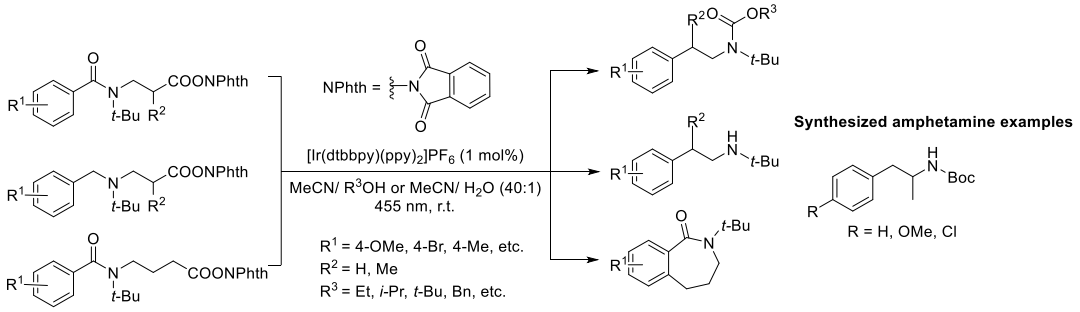

Scheme 26 Alkyl decarboxylative Smiles example of N-(acyloxy)phthalimides

Greaney *et al.* presented a method to access pharmacologically attractive substituted and unsubstituted aryl ethyl amine derivatives via the decarboxylative radical Truce-Smiles rearrangement using readily available β-amino acids *(Scheme 27)*.[45] The oxime esters were prepared by a simple condensation between ketoxime and alkyl carboxylic acids and the Smiles arylation began with an energy transfer process from the photoexcited Ir(III) catalyst to these oxime esters to give a biradical intermediate. The N-O bond could then be cleaved homolytically, releasing iminyl radical and carboxylate radical intermediates. Subsequent decarboxylation would generate the alkyl radical that could proceed to do the radical Smiles rearrangement yielding aryl ethylamine products.

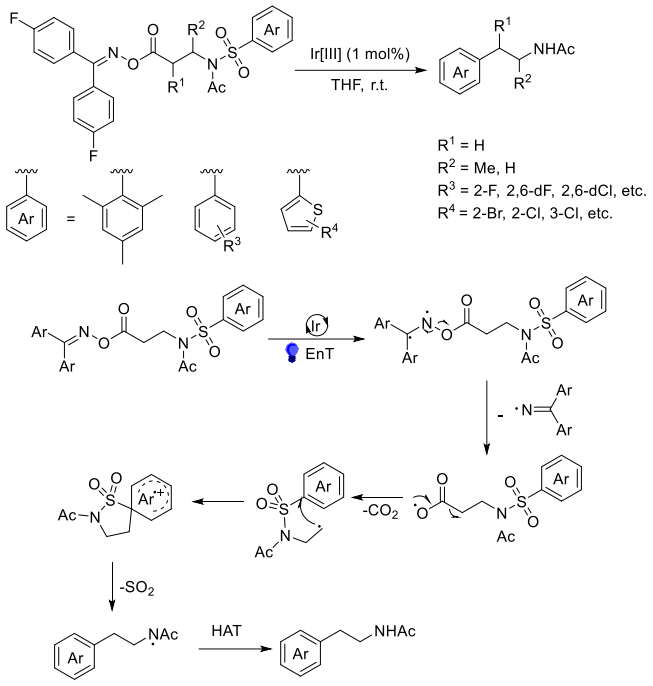

Scheme 27 Decarboxylative Smiles example of carbonyl oxime derivatives

Radical Smiles rearrangement of aryl benzoic acids

The sp^3-sp^2 radical Smiles coupling using alkyl carboxylic acids is more established than the coupling using aryl carboxylic acids due to the facile generation of alkyl radicals *(Section 2.1 on page 22)*. On the other hand, sp^2-sp^2 aryl-aryl Smiles coupling reactions from aryl carboxylic acid derivatives are less well explored, presumably due to the stable character of the aryl carboxylic acid presenting a big challenge for aryl radical formation. Often when using unactivated benzoic acids, another competitive pathway would dominate and rather than decarboxylating and generating the aryl radical, the carboxylate radical formed would behave as a nucleophile to react further *(Scheme 28)*. Jana and Hossian[46] demonstrated a silver(I)-catalyzed Smiles rearrangement on 2-aryloxy- and 2-arylthio- benzoic acid to afford aryl-2-hydroxybenzoate and aryl-2-mercaptabenzoate dimers. The benzoate radical did not decarboxylate even when harsh conditions such as high temperatures were used. Later, Gonzalez-Gomez *et al.*,[47] Li *et al*.,[48] and Yatham *et al.*[49] reported independently an O to O atom aryl transfer on 2-aryloxybenzoic acids to produce salol products using mild visible-light photoredox catalysis. In our work, we suggest that the recent discovery of aryl radicals

formed from the in-situ generation of aryl carboxylate-hypobromites[26] may overcome the challenges in aryl decarboxylative Smiles by using the sulfonylamido-benzoic acid substrate class.

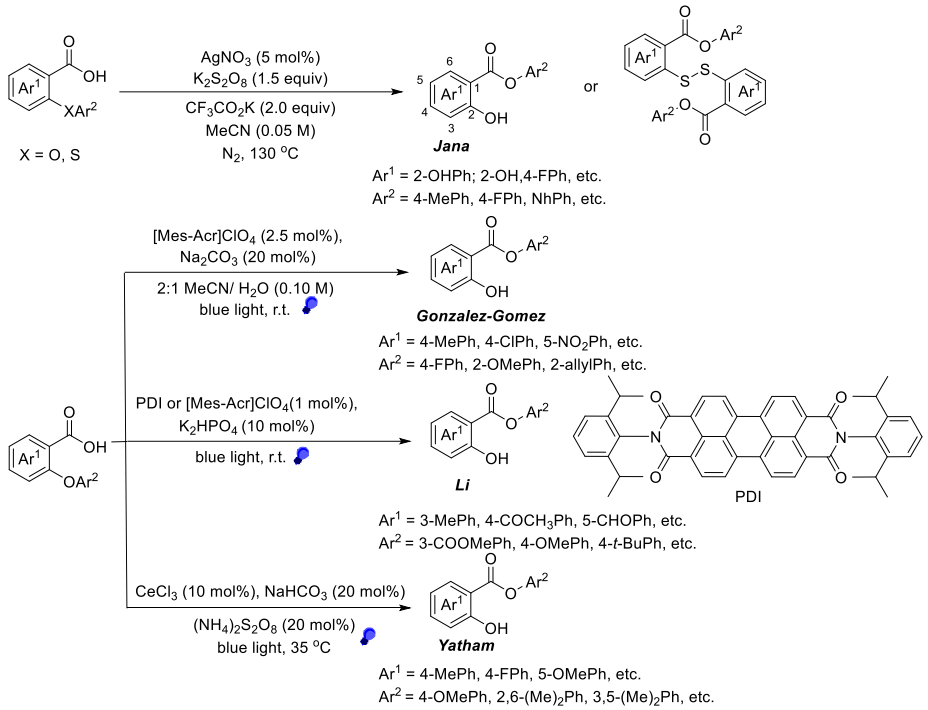

Scheme 28 Radical Smiles examples of aryl carboxylic acid functionalization

2.5 Strain-release ring-opening upon oxime N-O bond cleavage via photoredox catalysis

Strain-release ring-opening is an interesting approach in generating alkyl radicals and can be combined with iminyl radical generation. The iminyl radical generation usually involves the N-O homolysis from a ketoxime derivative due to the low N-O bond energy (BDE~50 kcal mol^{-1}).[50] Driven by the release of ring strain of a four-membered ring, the iminyl radical triggers a strain-release ring-opening to generate a distal cyano alkyl radical that allows for various functionalizations.[51] On top of the ubiquity of the nitrile group, the easy post-functionalization further enhances the synthetic utility of this method.[52]

Zard *et al*. reported the first deconstructive functionalization via iminyl radical generated from N-S bond fission using stoichiometric *n*-Bu_3SnH as the reductant.[53] Soon after, Zard demonstrated the N-O bond cleavage via the Barton

decarboxylation[54] and reductive opening via nickel powder[55]. Recently, research on N-O cleavage and functionalization has expanded rapidly due to the aid of transition metal catalysis *(Scheme 29a)*. Selender,[56] Umera,[57] Zhao and Shi,[58], Guo[59] demonstrated the use of Fe, Ir, Cu and Ni transition metal species to generate iminyl radicals that foster the β-C-C bond cleavage and subsequent functionalization *(Scheme 29b)*.

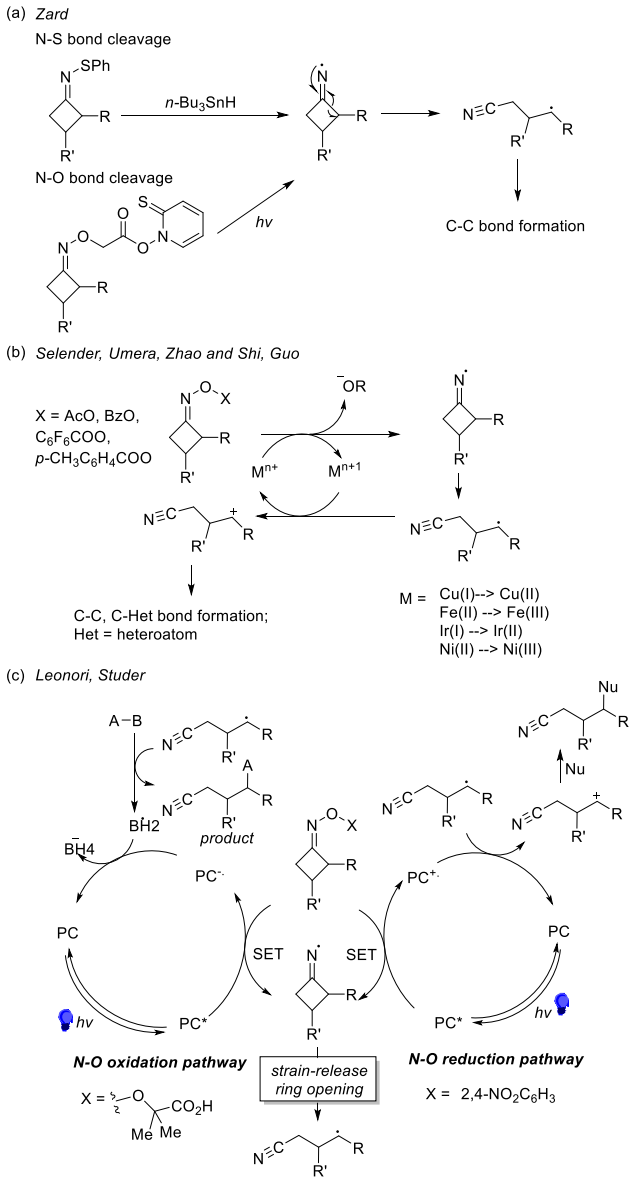

Scheme 29 Distal cyano-functionalization via cyclobutyl oxime N-O bond cleavage using (a) stoichiometric n-Bu_3SnH reductant; (b) transition-metal catalysis; (c) photoredox catalysis

Unlike the transition metal catalysed approach, photoredox catalysis allows both oxidative and reductive cleavage of the N-O bond, which allows access to a greater variety of substrates *(Scheme 29c)*.

Leonori, An, and Yu[60] first presented the functionalization of the iminyl radical via reductive fragmentation of the oxime N-O bond. Inspired by the early work of Zard via UV activation,[53, 61] Leonori[62] and Studer[63] separately reported the N-O scission triggered β-C-C bond cleavage via the oxidative pathway, which allows for the toleration of different functionalities. Harnessing the alkyl radical generated upon β-C-C bond cleavage of the strained cycloketoxime, Xiao, Wang, and Zhou demonstrated the tandem sp^3-sp^3 C-C bond formation.[64]

Recently, Greaney *et al*.[65] used this type of alkyl radical generation in the radical Truce-Smiles rearrangement to give arylethylamine products *(Scheme 30)*. The example of this Smiles rearrangement[65] and the various examples of deconstructive C-C bond functionalization by adding the alkyl radical to the Michael acceptor[64] prompted us to explore the tandem radical Smiles rearrangement using this radical generation. The distal cyano alkyl radical Smiles may allow access to valuable aryl propyl amine structures.

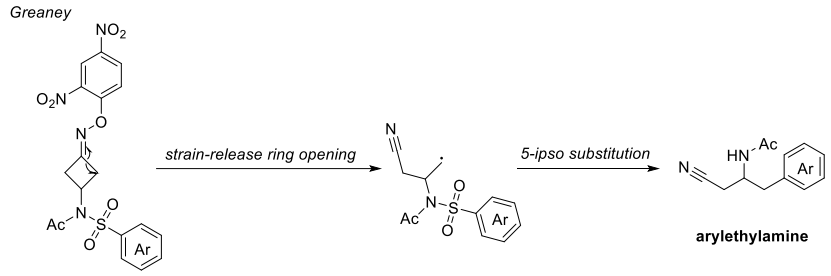

Scheme 30 Radical Smiles example of cyclobutyloxime derivatives

Chapter 3 Design and Methodology

3.1 Visible-light mediated radical Smiles aryl-aryl coupling

Anthranilic acid and salicylic acid are cheap and commercially available starting materials used in organic synthesis. We are interested in using these readily available anthranilic acid and salicylic acid derivatives **2.1** – **2.3** as starting materials *(Scheme 31)*.

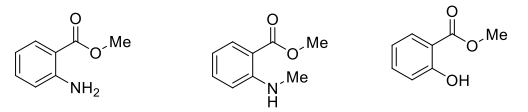

Scheme 31 Selected benzoic acid derivatives starting material

Recently there have been reports on aryl radical formation from benzoic acid, followed by its coupling with arenes and heteroarenes *(see Scheme 14, page 26)*.[26] Inspired by induced aryl decarboxylation from in-situ generated hypobromite intermediates using visible light, we propose a radical decarboxylative aryl-aryl coupling via a Smiles-rearrangement using sulfonylamido- or sulfonyloxy- benzoic acid **2.4** *(Scheme 32)*. After deprotonation of the benzoic acid **2.4**, benzoate anion **I** will be oxidized to give benzoate radical **II**. The bromine source will then react with the benzoate radical **II** to give hypobromite intermediate **III**, which will turn over the iridium catalyst [IrII] through an oxidation. The reduced hypobromite anion **IV** will undergo decarboxylation and give aryl radical intermediate **V**. Harnessing the non-sterically sensitive character of the radical-Smiles rearrangement, we envisioned that the decarboxylative aryl radical formed can be trapped by an intramolecular aryl group to achieve aryl-aryl coupling and give **VI**, which will give the biaryl product **2.5** after hydrogen atom transfer.

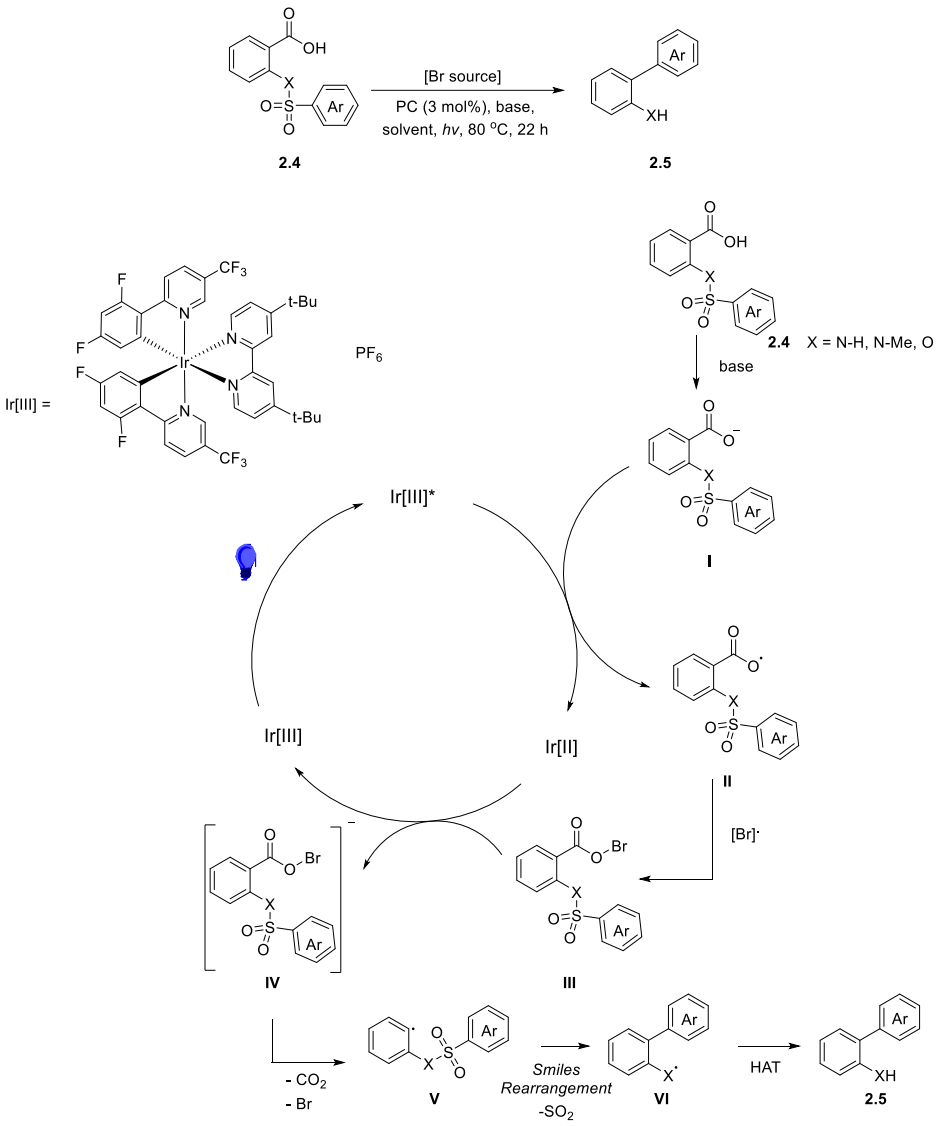

Scheme 32 Proposed photoredox pathway for aryl-aryl Smiles coupling

Sulfonamides are known to be favourable for 1,5-*ipso*-substitution in the radical Smiles rearrangement.[28, 30] To commence our study, we propose substrates **2.4.1 – 2.4.3** for the photoredox approach *(Scheme 33)*. The fluorine substituents are used as labels to indicate the formation of the rearrangement products.

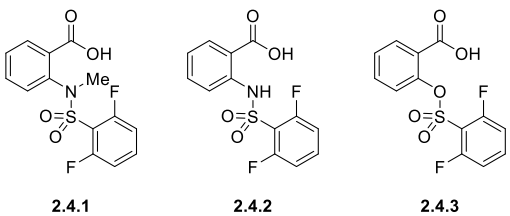

*Scheme 33 Benzoic acid substrates **2.4.1** -**2.4.3** for aryl decarboxylative radical Smiles rearrangement*

3.2 Strain-release cyclobutane ring-opening tandem radical Smiles rearrangement

The pioneering examples of Sapi[33] and Greaney[65] on the Truce-Smiles rearrangement encouraged us to examine the tandem cyclization radical Smiles reaction following a radical based strain release ring-opening reaction.[64]

We propose that the alkyl radical generated from the photocatalysed reductive N-O cleavage and strain-release ring-opening of the cyclobutene oxime derivative[64-65] would be compatible with a further Smiles rearrangement *(Scheme 34)*. The primary alkyl radical generated may be directed to the activated electron-deficient alkenes **3.5** and **3.6** generating a secondary alkyl radical after addition. This radical would then undergo a Truce-Smiles rearrangement to give cyclized arylpropylamine derived Smiles product **3.10**, a moiety with interest in medicinal chemistry.[66]

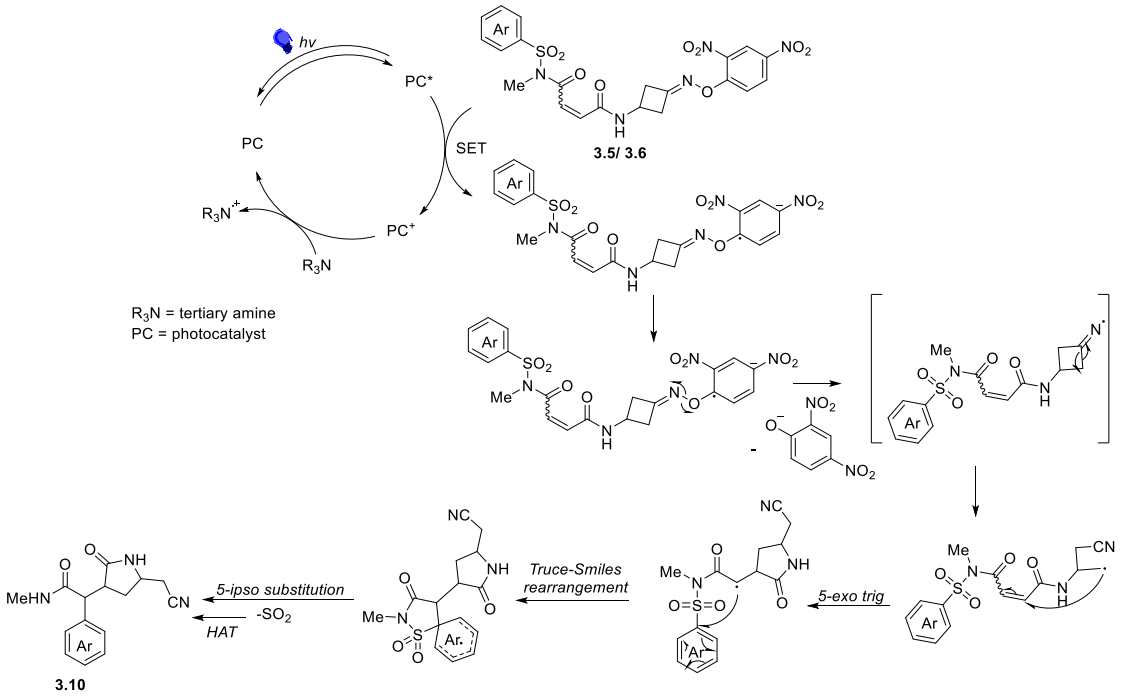

Scheme 34 Proposed catalytic pathway for intramolecular tandem Smiles rearrangement initiating by oxime N-O bond cleavage

We are interested in both the *cis*- and *trans*- configurations of the alkene as the isomer could have an influence on the stereochemistry of the new carbon centre generated at

the α-position of the amide after the radical Smiles rearrangement. We thereby propose both isomers **3.5** and **3.6** to investigate this tandem reaction *(Scheme 35)*.

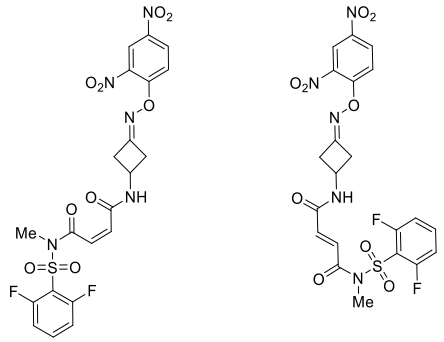

*Scheme 35 Proposed substrates **3.5** and **3.6** for intramolecular tandem Smiles rearrangement*

3.3 Alkyl decarboxylative Michael-addition type aryl migration

The pioneering examples of alkyl *N*-hydroxyphthalimide ester decarboxylation via photoredox catalysis and the addition of the generated alkyl radicals to Michael acceptors[16-17] guided us to combine the facile radical generation with sulfonyl methacrylamides to investigate the possibility of the intermolecular radical Smiles rearrangement.

Starting with single-electron reduction on the alkyl *N*-hydroxyphthalimide ester **4.1** using the photocatalyst,[16-17] radical decarboxylation of **4.2** would generate the alkyl radical *(Scheme 36)*. We envisage that the nucleophilic alkyl radical will add to the electron-deficient Michael acceptor in sulfonyl acrylamide **4.3** and give alkyl radical **4.4. 4.4** will then undergo the Truce-Smiles rearrangement yielding an amidyl radical. Finally, after hydrogen abstraction from the solvent or a trialkyl amine base, valuable product **4.5** with an α-quaternary carbon centre could be obtained.

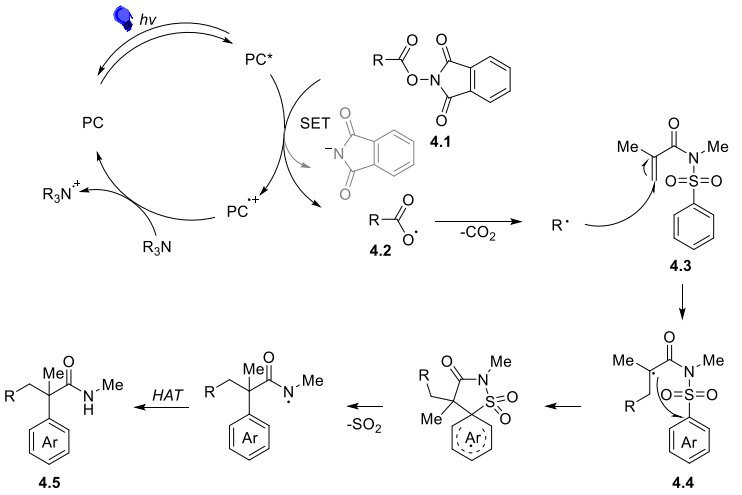

Scheme 36 Proposed alkyl decarboxylative intermolecular tandem radical Smiles rearrangement on sulfonyl methacrylamide

Methacrylamide **4.6** and cyclohexyl *N*-hydroxyphthalimide ester **4.7** are proposed as the Michael acceptor and the alkyl radical precursor to begin our study *(Scheme 37)*.

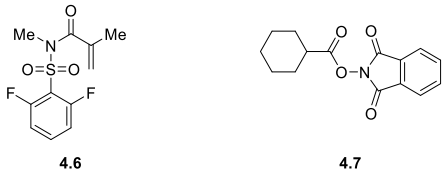

*Scheme 37 Proposed structure of methacrylamide **4.6** and cyclohexyl N-hydroxyphthalimide ester **4.7***

Based on our previous investigation on the Michael acceptor *(See Section 4.2)*, methacrylamide was used instead of acrylamide to enhance the stability of the alkene in our substrate **4.6**. The secondary alkyl radical generated from **4.7** would be relatively stable and nucleophilic, and has already been used in various Michael additions in the literature.[17b, 17d-k] To investigate the viability of this tandem reaction, we will begin our study with molecules **4.6** and **4.7**.

3.4 Reaction Monitoring

The high receptivity and large chemical dispersion of ^{19}F NMR spectroscopy makes it a useful way of monitoring the coupling reactions of fluorine-containing substrates.[67] We first reproduced the coupling reaction of one of the known substrates[26] to

confirm the change in the chemical shift in the ^{19}F NMR spectrum after aryl coupling *(Scheme 38)*. Resonances were observed at δ -108.19 ppm in the ^{19}F NMR spectrum (unreacted starting material) while peaks at δ -119.11 ppm arose from to the aryl coupled product. The significant chemical shift in the ^{19}F resonance (Δ ~10 ppm) after the *ortho*-aryl coupling prompted us to use crude ^{19}F NMR to observe the formation of coupled product.

Crude ^{19}F NMR spectrum (376 MHz, $CDCl_3$): δ (ppm) -108.19 (ddd, *J* = 10.7, 7.2, 4.8 Hz), -118.11 (dddd, *J* = 12.9, 6.4, 3.4, 1.7 Hz).

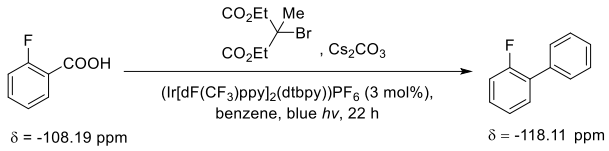

Scheme 38 Visible-light mediated decarboxylative aryl coupling of 2-fluorobenzoic acid

In this regard, the 2,6-difluorobenzene moiety was incorporated into most of our substrates as a quick tool to analyse the reactions.

Chapter 4 Results and Discussion

4.1 Visible-light mediated radical Smiles aryl-aryl coupling

Several sulfonylamido and sulfonyloxy benzoic acids were synthesized and investigated for the visible-light mediated aryl-decarboxylative radical Smiles rearrangement. Inspired by the photoredox generation of aryl radicals through decarboxylation, different conditions were applied to study the viability of decarboxylative aryl-aryl coupling via a radical Smiles rearrangement.

Sulfonamides and sulfonates were synthesized through a short two-step procedure *(Scheme 39)*. Dimethyl anthranilate **2.1**, methyl anthranilate **2.2**, and methyl salicylate **2.3** were reacted with aryl sulfonyl chlorides in presence of pyridine or triethylamine base to afford sulfonylamido and sulfonyloxy benzoate intermediates **2.7**. Benzoate esters **2.7** were then hydrolyzed to the benzoic acids with lithium hydroxide. The three benzoic acid substrates **2.4.1** to **2.4.3** obtained after hydrolysis were used in the photoreactions.

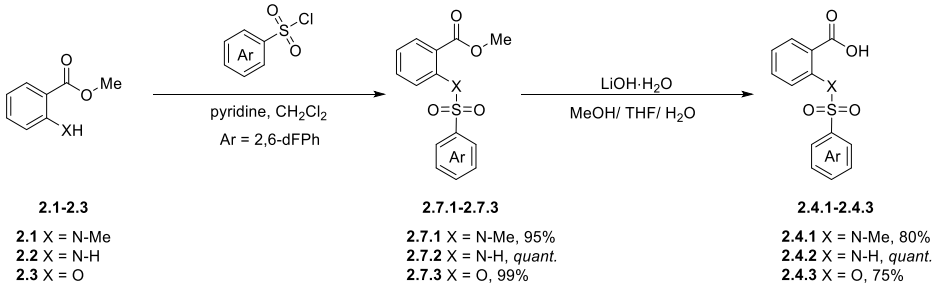

*Scheme 39 Synthetic pathway of **2.4.1**-**2.4.3***

We propose **2.4.1** to **2.4.3** would decarboxylate under mild photochemical conditions as described in *Section 3.1* to generate an aryl radical, which would then perform a Smiles rearrangement to form the aryl-aryl bond *(Scheme 40)*.

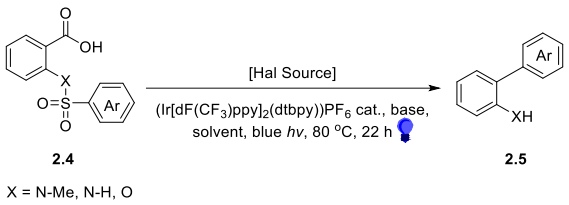

Scheme 40 Decarboxylative aryl-aryl coupling using radical Smiles rearrangement

To begin our proposed decarboxylative Smiles reaction *(Scheme 40)*, we initially began with the conditions[26] developed by F. Glorius and co-workers on **2.4.1** and **2.4.2** *(Table 2, entry 1, and Table 3, entry 6)*. The reactions were monitored by ^{1}H and ^{19}F NMR spectroscopy, where an internal standard was not used in the ^{19}F NMR spectra. No reaction was observed by following the literature conditions. We suspected that the lack of reactivity might be attributed to the poor solubility of the benzoic acid, therefore solvent screening was performed.

No reaction was observed for the different solvents tried *(Table 2)*. There are various possible reasons for the unsuccessful decarboxylation. Ineffective deprotonation of the substrate due to substrate solubility, changes in acidity of the carboxylic acid in different solvent, or other undesired events such as back electron transfer or HAT *(See section 2.1 on page 24)* could lead to unsuccessful decarboxylation.

*Table 2 Solvent screen of **2.4.2***

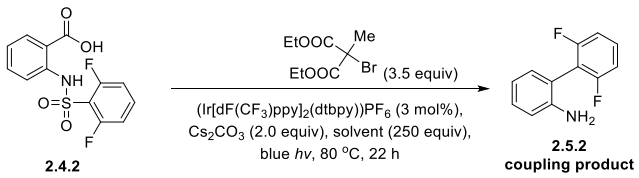

Entry	Solvent	Result
1	benzene/ MeCN[a]	n.r.
2	MeCN	n.r.
3	THF	n.r.
4	DMF	n.r.
5	DMSO	n.r.

[a] benzene/acetonitrile (molar ratio 3:5) in 400 equivalents relevant to the **2.4.1** was used as the solvent. Reaction was conducted at 55 °C.

In the first step of decarboxylative radical generation, the benzoic acid must be deprotonated *(Scheme 32)*. In our substrate, however, there was also an acidic sulfonamide N-H proton present[68] which might be competitively deprotonated. Therefore, we repeated the solvent screening on substrates **2.4.1** and **2.4.3** which do not have this competitive deprotonation possibility *(Table 3)*. However, we only obtained starting material under these conditions.

*Table 3 Solvent screen of **2.4.1** and **2.4.3***

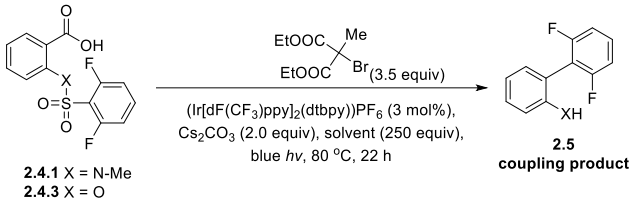

Entry	Substrate	Solvent	Result
6	2.4.1	MeCN	n.r.
7	2.4.1	THF	n.r.
8	2.4.1	DMF	n.r.
9	2.4.1	DMSO	n.r.
10	2.4.3	MeCN[b]	n.r.
11	2.4.3	benzene	n.r.

[b]50 equivalents of solvent was used.

At this point, we resynthesized **2.4.1** on an increased scale (5 mmol), but at this scale, there was a noticeable unidentified side product shown in the ^{1}H NMR spectrum, which was unable to be removed by column chromatography. Thus, for the next steps, we decided to continue screening using **2.4.2** and trying different inorganic and organic bases. On account of our substrate having good solubility in acetonitrile, which is also known as unfavourable for HAT,[69] acetonitrile was chosen as the solvent to continue the condition screening on **2.4.2**.

When using KOAc, no reaction was observed *(Table 4, entry 12 – 13)*. Whereas when phosphate bases or CsF were used, trace amounts of suspected decarboxylation product **2.6.2** were observed as indicated by ^{19}F NMR and mass spectrometry *(entries 14 – 16)*. We proposed that **2.6.2** is formed from decarboxylation of **2.4.2** followed by hydrogen abstraction from the solvent.

*Table 4 Inorganic base screen on **2.4.2***

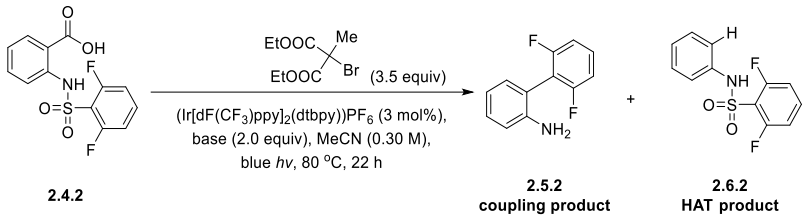

Entry	Base	Coupling product[e]	HAT product[e]
12	KOAc	/	/
13[c]	KOAc	/	/
14	K_3PO_4	/	trace
15	K_2HPO_4	/	trace
16	CsF	/	trace

[c]The halogen source, diethyl 2-bromo-2-methylmalonate (0.30 M), was used as solvent.
[e]The results (in %) reported referred to the amount of product observed in ^{19}F NMR spectra relative to the benzoic acid starting materials **2.4.1-2.4.5**

Starting materials were all solubilized when organic bases were used. No HAT or coupling product was observed when stronger organic base DIPEA was used *(Table 5, entry 17)*. It was likely that the superstoichiometric amine base served as a reductant that reduced our Ir(III) catalyst to Ir(II), which competed with our desired oxidation of the carboxylate anion. Poor reactivity was seen with various other bases *(entries 18-21)*.

*Table 5 Organic base screen of **2.4.2***

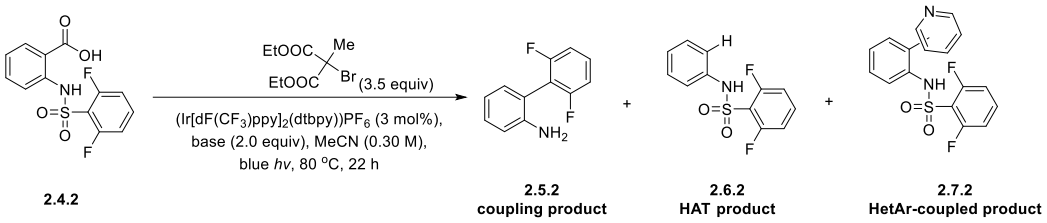

Entry	Base	Coupling product[e]	HAT product[e]	HetAr-coupled product[e]
17[d]	DIPEA	/	/	/
18	DBU	/	trace	/
19	DABCO	/	trace	/
20	Imizadole	/	trace	/
21	pyridazine	/	/	/
22	TMG	/	39%	/
23	pyridine	trace	38%	14%

[d]10.0 equivalents of base, 10.0 equivalents of halogen source was used. Concentration was conducted at 0.01 M. [e]The results (in %) reported referred to the amount of product observed in ^{19}F NMR spectra relative to the benzoic acid starting materials **2.4.2**.

When weaker bases TMG and pyridine were used, a significant amount of decarboxylation was observed *(Table 5, entries 22-23)*. The results (in %) reported in the tables referred to the amount of product observed in ^{19}F NMR spectra relative to the benzoic acid starting materials **2.4.1-2.4.5**. Interestingly, with the use of pyridine base, some of the aryl radical also coupled with the pyridine to give the HetAr-coupled mixture **2.7.2** with unknown regioselectivities, as well as the suspected HAT product **2.6.2**, and the Smiles coupling product **2.5.2** *(entry 23)*. In the ^{19}F NMR spectrum, three major sets of peaks at δ-105.93, -108.84, -108.94 correspond to **2.7.2**, **2.6.2**, and **2.4.2**, while a small set of peaks at δ -113.38 was suspected to be the Smiles product **2.5.2** due to the significant change in the chemical shift. From the ESI-HR MS results, the masses of **2.5.2**, **2.6.2**, and **2.7.2** were found to be [M] = 205.0698, $[M+Na]^+$ = 369.0480, and $[M+Na]^+$ = 292.0214.

We went forward with the use of pyridine base, while changing the ratios of reagents and concentrations hoping to optimize the conditions. In an attempt to achieve more

efficient deprotonation, we carried out the reaction in neat pyridine *(Table 6, entry 24)*, but no enhanced decarboxylation was observed. A moderate amount of decarboxylation HAT product was observed when the pyridine base was lowered to 1.2 equivalents *(entry 25)*. In the suspicion that a high reaction concentration would favour the intermolecular formation of the Het-Ar coupled product **2.7.2** *(Table 5, entry 23)*, the concentration of the reaction was lowered to reduce these intermolecular coupling events *(Table 6, entries 27-29)*. However, we still observed 26% of the HAT product **2.6.2** indicating that there was a different issue that hindered the aryl Smiles reaction *(entry 27)*.

Table 6 Variation from entry 23 (Concentration and ratio of reagents)

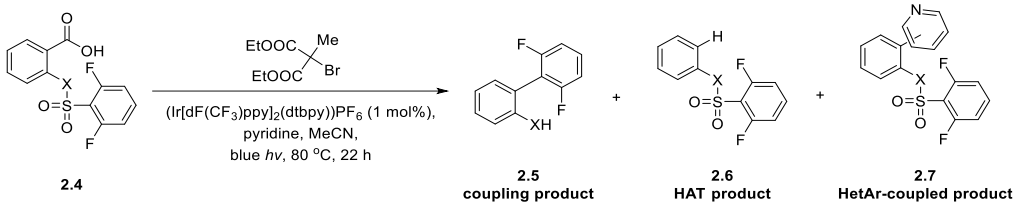

Entry	Substrate	Base (equiv)	Bromine Source (equiv)	Conc. (M)	Coupling Product[e]	HAT Product[e]	HetAr-coupled product[e]
24	2.4.2	neat	3.5	0.30	/	trace	trace
25	2.4.2	1.2	3.5	0.30	trace	24%	trace
26	2.4.2	3.0	2.0	0.01	trace	trace	trace
27	2.4.2	2.0	3.5	0.10	trace	26%	trace
28	2.4.2	2.0	2.0	0.02	trace	trace	/
29	2.4.2	2.0	2.0	0.01	trace	trace	/
30	2.4.1	2.0	10.0	0.01	/	24%	/
31	2.4.3	2.0	10.0	0.01	/	/	/
32[f]	2.4.2	2.0	10.0	0.01	trace	trace	trace
33	2.4.2	2.0	10.0	0.05	/	/	trace
34	2.4.2	2.0	10.0	0.01	trace	40%	trace
35[g]	2.4.2	2.0	10.0	0.05	trace	trace	trace
36[g]	2.4.2	2.0	10.0	0.01	/	trace	26%

[e]The results (in %) reported referred to the amount of product observed in ^{19}F NMR spectra relative to the benzoic acid starting materials **2.4**. [f]CD_3CN was used as solvent. [g]Reaction was conducted at room temperature.

Although acetonitrile was known to be reluctant to donate a hydrogen atom,[69] we suspected the large amount of solvent molecules or the N-H group present in **2.4.2** could be the hydrogen source for the HAT product **2.6.2**. As a potential hydrogen source donor and competitor in the deprotonation of carboxylic acid, the N-H moiety seemed to be problematic. However, changing substrate to **2.4.1** and **2.4.3** only gave 24% HAT product **2.6.1** *(Table 6, entry 30)*, where no reaction was observed for sulfonate **2.4.3** *(entry 31)*. Deuterated solvents were known to slow down the hydrogen atom donation[22] due to the kinetic isotope effect and when deuterated acetonitrile was used, only trace amount of HAT product **2.6.2** was observed, but still no significant Smiles product was observed *(entry 32)*. Meanwhile, we suspected the superstoichiometric bromomethyl malonate used in the literature served as an oxidant that could turn over the catalytic cycle. Keeping reaction concentration at 0.01 M at 80 ^{o}C, when the bromine source was increased to 10.0 equivalents, 40% of HAT product **2.6.2** was observed *(entry 34)*, and 26% of HetAr-coupled product **2.7.2** was observed by conducting the reaction at room temperature *(entry 36)*. While when the reaction was conducted at 0.05 M, little or no decarboxylation product was found (*entries 33 and 35*). Since no significant amount of coupling product **2.5** was observed by any deviation in condition or changing the substrate *(Table 6)*, we proceeded to investigate the reaction using **2.4.2** with different pyridine derivatives.

When more electron-deficient pyridines were used *(Table 7, entries 37 - 38)*, almost no reaction was observed, whereas when more electron-rich pyridines were used, more decarboxylation events were observed *(entry 39 – 41)*. Despite the enhanced efficiency in aryl decarboxylation, no significant Smiles products were observed and a mixture of HAT and HetAr coupled products were observed. We hoped that the intermolecular coupling of the aryl radical onto our pyridine would be suppressed by reducing the concentration of the reaction. Therefore, we reduced the concentration of **2.4.2** from 0.30 M to 0.01 M in the following halogen source screening *(Table 8)*.

*Table 7 Screening of pyridine-derived base on **2.4.2***

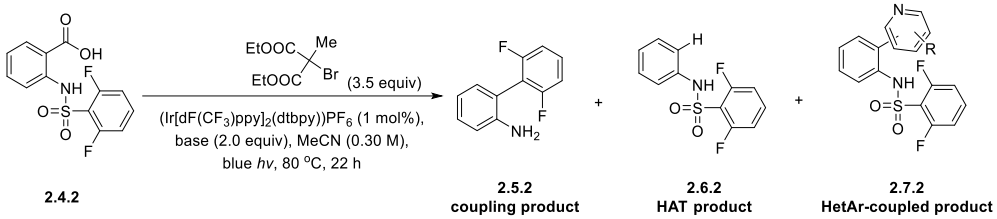

Entry	Base	Coupling Product[e]	HAT Product[e]	HetAr-coupled product[e]
37	3-nitropyridine	/	/	/
38	3-bromopyridine	/	/	trace
39	2,6-lutidine	/	30%	trace
40	4-tertbutylpyridine	/	39%	19%
41	4-methoxypyridine	/	15%	38%

[e]The results (in %) reported referred to the amount of product observed in ^{19}F NMR spectra relative to the benzoic acid starting materials **2.4.2**.

Given the significant amount of HAT products and HetAr mixture again with unknown regiochemistry observed, we rationalized that deprotonation and radical generation was at least partially successful. Next, we looked at different halogen sources used in generating the hypohalite intermediate that would facilitate the decarboxylation. From our experiments, bromine was an adequate substitute for **H1** *(Table 8, entry 42)*, while little or no decarboxylation was found when other halogen sources were used *(entries 43 - 47)*.

Table 8 Halogen source screening

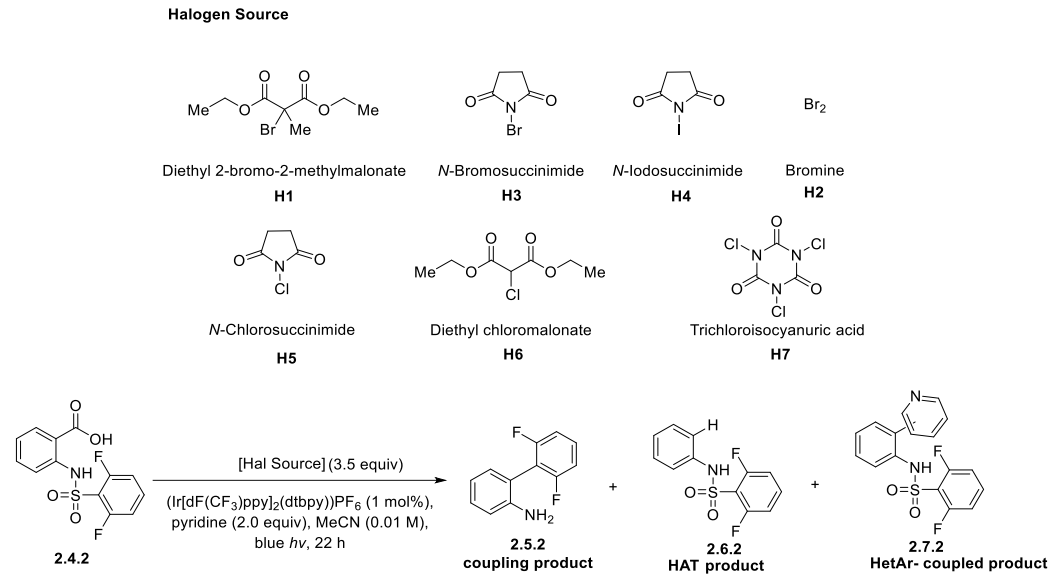

Entry	Halogen source	Temp (°C)	Coupling product[e]	HAT product[e]	HetAr-coupled product[e]
42	H2	55	trace	29%	37%
43	H3	80	/	/	trace
44	H4	80	/	/	/
45	H5	55	/	trace	/
46	H6	80	/	/	/
47	H7	80	trace	/	/

[e]The results (in %) reported referred to the amount of product observed in ^{19}F NMR spectra relative to the benzoic acid starting materials **2.4.2**.

Inspired by Han *et al*.,[29] a mesityl sulfonamide derivative was shown to be successful in a radical Smiles reaction to form aryl-aryl bonds. According to their scope, sulfonamides with electron-rich arenes gave a better yield, which may be attributed to the successful trapping of the electron-deficient aryl radical. Therefore, we synthesized **2.4.4** and **2.4.5** *(Scheme 41)*, which contain less electron-deficient arenes, and attempted the reactions using the conditions where trace Smiles product was observed in our study.

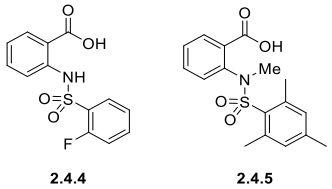

*Scheme 41 Sulfonamide substrate **2.4.4** and **2.4.5** with less electron-deficient arenes*

Despite more decarboxylation events when a less electron-deficient arene was used *(Table 9, entry 48)*, no Smiles coupled product was observed. Starting material **2.4.5** degraded and no significant amount of decarboxylative coupled product could be isolated in flash column chromatography *(entry 49)*, possibly because the benzylic methyl substituents are good hydrogen atom donors.

*Table 9 Visible-light mediated aryl decarboxylative reaction on **2.4.4** and **2.4.5***

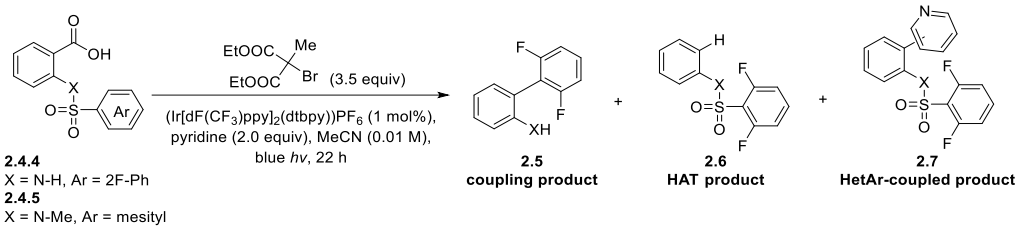

Entry	Substrate	Halogen source	Coupling product[e]	HAT product[e]	HetAr-coupled product[e]
48	2.4.4	3.5 equiv	/	42%	trace
49	2.4.5	10.0 equiv	/	/	/

[e]The results (in %) reported referred to the amount of product observed in ^{19}F NMR spectra relative to the benzoic acid starting materials **2.4.4** and **2.4.5**

Finally, a photosensitized approach[24] was adapted to avoid the problem of acid deprotonation, where an activating group 4-fluorobenzylketoxime was added to the benzoic acid **2.4.5**. **2.8** was synthesized by condensing **2.4.5** and bis(4-fluorophenyl) methanone oxime using EDC as the coupling reagent *(Scheme 42)*. In this case, after energy transfer from the excited photocatalyst to the oxime ester, reduction of the active ester should be facile leading to a carboxylate radical. The result was confirmed by ESI-MS, no starting material or Smiles product was detected, only corresponding benzoic acid was observed, which suggested the cleavage of N-O bond without any

subsequent aryl decarboxylation, which was consistent with the result in the literature[24] that decarboxylation was inefficient in arenes with an *ortho*-substituent.

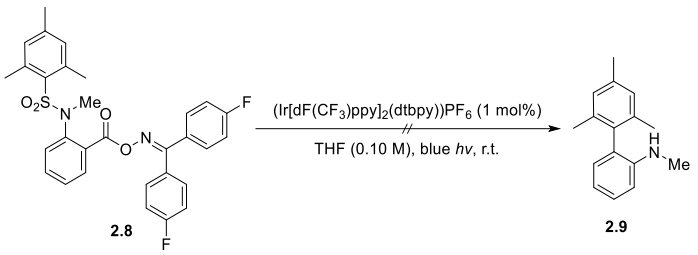

*Scheme 42 Photosensitized aryl decarboxylation of **2.8***

4.2 Strain-release cyclobutane ring-opening tandem radical Smiles rearrangement

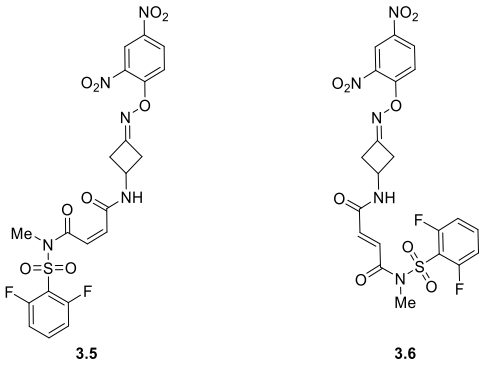

*Scheme 43 Cyclobutyloxime substrates **3.5** and **3.6** for tandem radical Smiles rearrangement*

For the tandem Smiles rearrangement reaction, we first attempted the synthesis of *trans*-alkene substrate **3.6** *(Scheme 44)*.

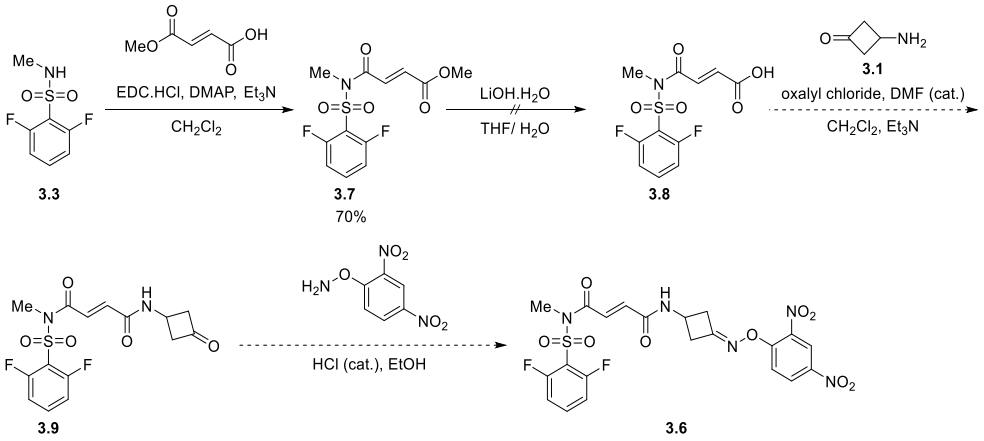

*Scheme 44 Synthetic scheme I for **3.6***

Beginning with amide coupling, **3.3** was reacted with mono-methyl fumarate using EDC·HCl to afford **3.7** in 70% yield. However, during hydrolysis to **3.8**, both the sulfonamide and the methyl ester were found to be hydrolyzed.

To avoid this regioselectivity problem, 3-aminocyclobutan-1-one **3.1** was first conjugated to mono-methyl fumarate *(Scheme 45)*. Unfortunately, the amide and the methyl ester in **3.11** were found to be hydrolyzed. For both **3.7** and **3.11**, exposure to milder inorganic bases such as KOH and NaOH for shorter reaction times and under lower temperatures gave the same result.

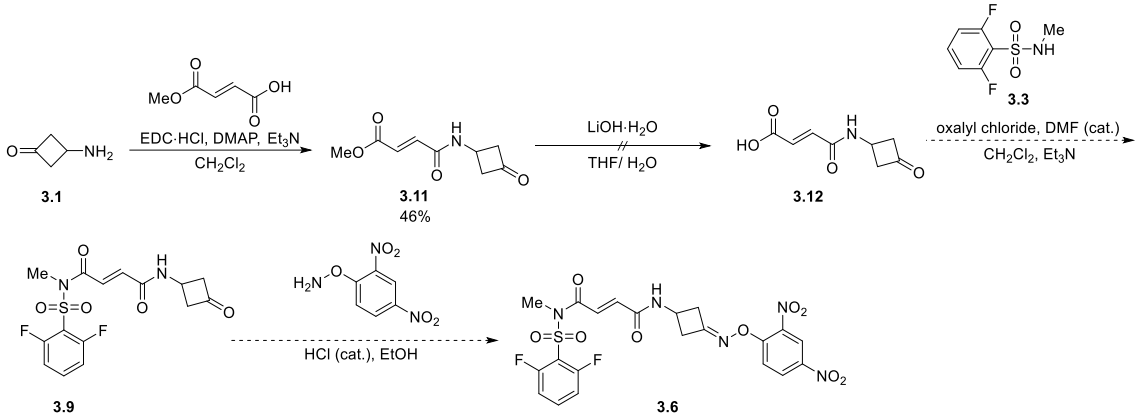

*Scheme 45 Synthetic scheme II for **3.6***

Given the difficulty in working with the *trans*-alkene, we decided to attempt to synthesize the *cis*-alkene **3.5** through a pathway that avoid problematic hydrolysis steps *(Scheme 46)*. Carboxylic acid **3.2** was synthesized using **3.1** to open maleic anhydride in the presence of triethylamine base. The amide coupling between carboxylic acid **3.2** and sulfonamide precursor **3.3** proceeded using 1-ethyl-3-carbodiimide hydrochloride as the coupling reagent to afford **3.4** in moderate yield. Condensation between **3.4** and corresponding hydroxylamine afforded pure substrate **3.5** in 48% yield after simple suction filtration.

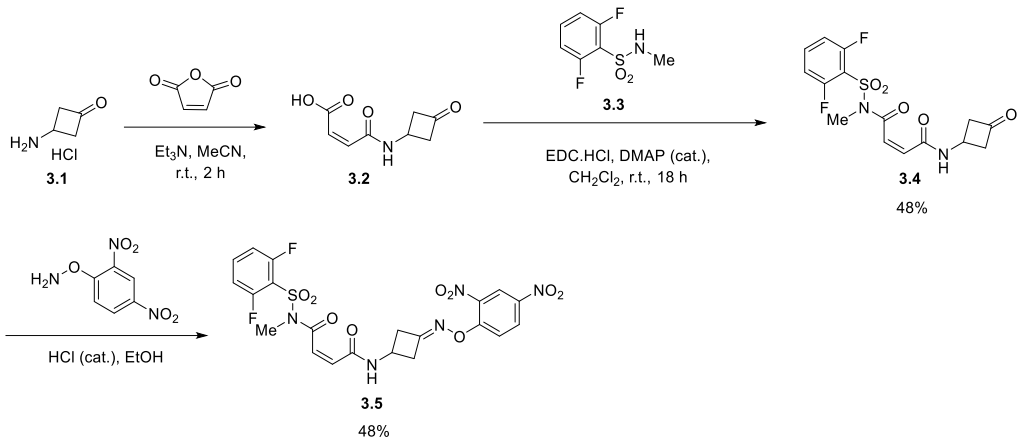

*Scheme 46 Synthetic scheme for **3.5***

Our starting point for the photocatalytic tandem Smiles were the optimized conditions used in the strain-release system in Greaney's work.[65] Unfortunately, all starting materials became degraded *(Table 10, entry 1)*. We suspected this might be due to the substrate's incompatibility with the 1-methylpyrrolidine base. To continue to explore the tandem reaction, we attempted the photoreaction with more robust iridium catalysts $[Ir(dtbbpy)(ppy)_2]PF_6$ and $Ir(ppy)_3$ as well as a more hindered amine base. However, the same result was observed *(entries 2 - 3)*. A control experiment was conducted where 1-methylpyrrolidine base was stirred overnight with substrate **3.5** in dark at room temperature. Again, the starting material **3.5** was degraded *(entry 4)*, similar to when **3.5** was exposed to light *(entry 1)*. It has been previously shown that a catalytic amount of tertiary amine base could form Baylis-Hillman adducts that lead to subsequent addition reactions.[70] To avoid this possibility we tried the reaction with eosin Y as a stoichiometric reductant for the oxime N-O bond cleavage. However, the ^{1}H NMR spectroscopy on the crude showed most of the starting material remained intact indicating that neither the cyclobutane nor the alkene moiety had reacted. Therefore, we decided to study the photoreactions with more reducing iridium catalysts.

*Table 10 Photoreaction of **3.5** with tertiary amine reductants*

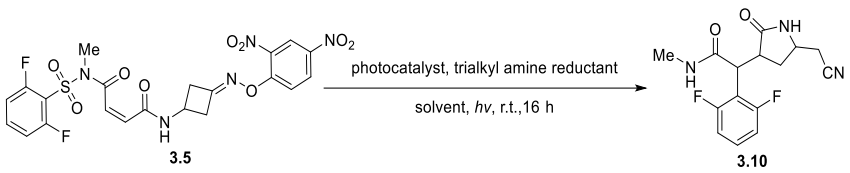

Entry	Reductant	Catalyst	Solvent	Light	Results
1	1-methylpyrrolidine (2.0 equiv)	eosin Y (5 mol%)	CH_2Cl_2 (0.05 M)	green	s.m. degraded
2	DIPEA (2.0 equiv)	$[Ir(dtbbpy)(ppy)_2]PF_6$ (2 mol%)	MeCN (0.05 M)	blue	s.m. degraded
3	DIPEA (2.0 equiv)	$Ir(ppy)_3$ (2 mol%)	MeCN (0.05 M)	blue	s.m. degraded
4	1-methylpyrrolidine (2.0 equiv)	/	CH_2Cl_2 (0.05 M)	dark	s.m. degraded
5	/	eosin Y (1 equiv)	MeCN (0.025 M)	green	n.r.

S.m. = starting material, n.r. = no reaction.

As ^1H and ^{19}F spectroscopy were mostly used for reaction monitoring, there is difficulty in concluding if the N-O cleavage has happened when we have a mixture of compounds present. In the reduction step of the oxime ester, the iminyl radical generated is nucleophilic and could abstract hydrogen readily.[62a] Therefore, we wanted to avoid reductants which were good HAT reagents.

Encouraged by the earlier work of Stephenson,[13, 71] we attempted the reaction with mild reductants which were shown to prevent early HAT events *(Table 11, entry 6 and 7)*. Despite being an efficient HAT agent, cyclohexadiene (CHD) has been shown to be an efficient reductant in completing the catalytic cycle when eosin Y was used as the photocatalyst in Leonori's work *(entry 8)*.[60a] Since our starting material **3.5** was shown to degrade despite using these milder reductants, we attempted a light-mediated N-O bond weakening via the formation of a noncovalent anion–π complex, using a milder inorganic base such as potassium carbonate *(entry 9)*.[72] Although the cyclobutane and the alkene had reacted by observation of the crude ^1H NMR spectra, no cyclization or

Smiles reaction was observed in the reaction. More importantly, the sulfonamide moiety was also cleaved in this reaction.

*Table 11 Reductant screening for **3.5***

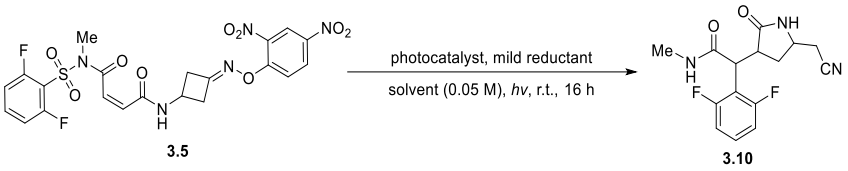

3.5 3.10

Entry	Reductant/ base	Catalyst	Solvent	Light	Result
6	$LiB(cat)_2$[a] (2.0 equiv)	$[Ir(dtppy)(ppy)_2]PF_6$ (2 mol%)	MeCN	blue	s.m. degraded
7	NEt_3/ formic acid (1.5 equiv)	$[Ir(dtppy)(ppy)_2]PF_6$ (2 mol%)	MeCN	blue	s.m. degraded
8	K_2CO_3/ CHD (2.0 equiv)	eosin Y (5mol%)	Acetone	green	s.m. degraded
9[b]	K_2CO_3 (2.0 equiv)	/	MeCN	blue	s.m. degraded

[a]$LiB(cat)_2$ referred to lithium bis-catechol borate. [b]Reaction was conducted in the absence of photocatalyst while K_2CO_3 was used as the anionic compartment in the formation of anion–π complex. S.m. = starting material.

Substrate **3.5** was found to be too reactive in the investigation of the tandem radical Smiles rearrangement. We believed this is due mainly to the electron-deficient alkene. The overreactive substrate **3.5** propelled us to study the intermolecular tandem Michael addition-radical Smiles reaction *(Section 4.3)*.

4.3 Alkyl decarboxylative Michael-addition type aryl migration

Sulfonyl acrylamide **4.6** was synthesized in a two-step, one-pot procedure *(Scheme 47)*. Methacrylic acid reacted with oxalyl chloride with catalytic DMF to generate **4.13** *in situ*, which was directly used for the coupling with sulfonamide **3.3** to afford **4.6** in 64% yield.[35b, 35c, 73]

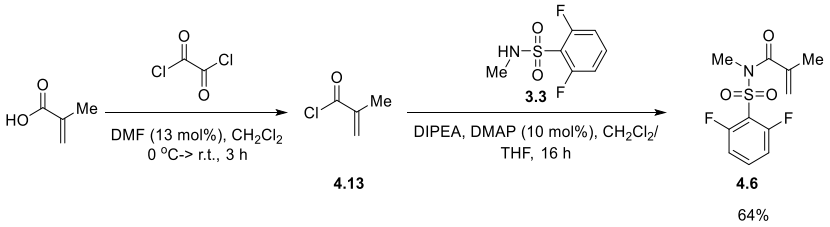

*Scheme 47 Synthetic scheme of **4.6***

N-Hydroxyphthalimide ester **4.7** was prepared by coupling cyclohexyl carboxylic acid with *N*-hydroxyphthalimide in presence of DCC and catalytic DMAP following a literature procedure *(Scheme 48)*.[17g]

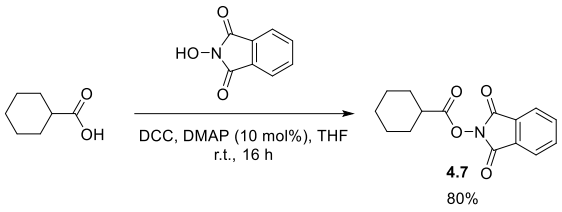

*Scheme 48 Synthetic scheme of **4.7***

Sulfonyl acrylamide **4.6** and phthalimide ester **4.7** were synthesized to investigate the intermolecular tandem Michael-addition Smiles reaction between **4.6** and **4.7**. The photoreaction was attempted with iridium photocatalysts and a tertiary amine base as the terminal reductant *(Table 12, entries 1 - 2)*. Later, we tried various conditions that have been previously used in the alkyl decarboxylation-Michael addition reaction *(entries 3 - 4)*. Since a tiny amount of Smiles product was observed in the crude ^{19}F NMR and ESI-mass spectrum and starting material was partly consumed, we altered the amount of trialkyl amine base and the alkyl *N*-hydroxyphthalimide ester **4.7** hoping to increase the Smiles product formation *(entries 5 – 7)*. At the same time, the reaction was attempted under increased concentrations, hoping to enhance the intermolecular addition of the alkyl radical to the alkene *(entries 5 – 7)*. However, it was observed that most of the starting material was in fact degraded. To combat this, we attempted this reaction at a lower concentration (0.02 M). Unfortunately, the crude reaction mixture still showed a similar degradation pattern based on the ^{1}H and ^{19}F NMR spectroscopic data *(Table 12, entry 8)*.

Table 12 Reagent portion variation

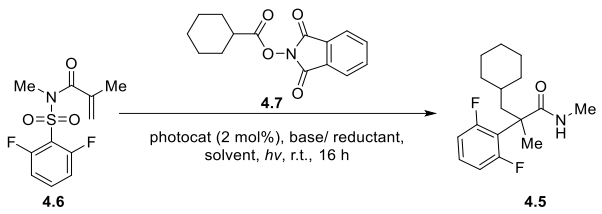

Entry	4.7 (equiv)	Reductant / base	Catalyst	Solvent	Light	Smiles product
1	1.5	DIPEA (2.0 equiv)	$Ir(dtbbpy)ppy_2PF_6$	CH_2Cl_2 (0.05 M)	blue	trace
2	1.5	DIPEA (2.0 equiv)	$Ir[dF(CF_3)ppy]_2(dtbpy)PF_6$	CH_2Cl_2 (0.05 M)	blue	trace
3[a]	1.5	DIPEA (2.0 equiv)	eosin Y[a]	CH_2Cl_2 (0.07 M)	green	trace
4[b]	1.5	K_3PO_4 (2.0 equiv)	*fac*-$Ir(ppy)_3$	$MeCN/H_2O$ (0.10 M)[b]	white	trace
5	1.5	DIPEA (2.0 equiv)	$Ir(dtbbpy)ppy_2PF_6$	CH_2Cl_2 (0.10 M)	blue	trace
6	3	DIPEA (2.0 equiv)	$Ir(dtbbpy)ppy_2PF_6$	CH_2Cl_2 (0.10 M)	blue	trace
7	3	DIPEA (3.0 equiv)	$Ir(dtbbpy)ppy_2PF_6$	CH_2Cl_2 (0.10 M)	blue	trace
8	1.5	DIPEA (2.0 equiv)	$Ir(dtbbpy)ppy_2PF_6$	CH_2Cl_2 (0.02 M)	blue	trace

[a] Photocatalyst (10 mol%) was used. [b]Reaction was conducted in a (9:1; v/v) mixture of MeCN/ H_2O.

Various possibilities for the observed degradation/poor reactivity are possible. Regarding the phthalimide ester **4.7**, it might be possible that the decarboxylation process was not effective, or the generated alkyl radical abstracts a hydrogen atom through a HAT process with the tertiary amine or solvent *(Scheme 49)*. Considering the sulfonyl acrylamide **4.6**, the alkene in **4.6** may be amine base sensitive such that the nucleophilic anion generated could trigger side reactions such as self-condensation. Furthermore, there might be undesired interactions between either the alkene or the relatively electron-rich nitrogen and the photoredox cycle that sets off a series of chain events which may hinder the addition of the alkyl radical from **4.7** to the alkene

(Scheme 49). Due to the multiple possibilities, we started by investigating some control experiments.

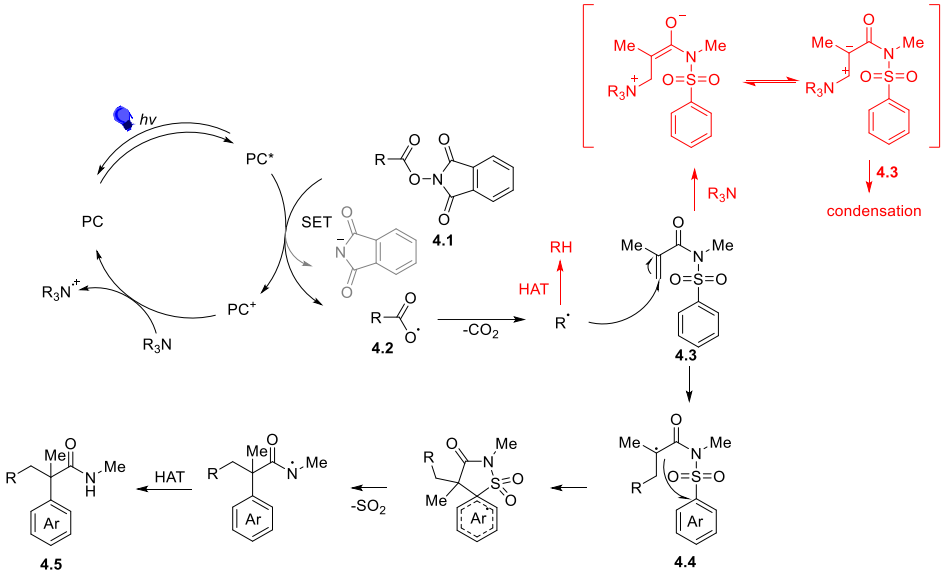

Scheme 49 Possible side events initiated by generated alkyl radical

Experiments were carried out on substrate **4.6** to investigate its stability. Compound **4.6** was stable when it was put with base in the dark (*Table 13*, entry 9) and with Ir(dtbbpy)ppy$_2$PF$_6$ (2 mol%) under blue light irradiation (*Table 13*, entry 10). When **4.6** was put through the reaction conditions in the absence of **4.7**, all of the alkene was reacted giving a mixture of unidentified degradation compounds (*Table 13*, entry 11). This suggested that substrate **4.6** was indeed interacting with the reactive components in the photoredox cycle.

Table 13 Control experiments

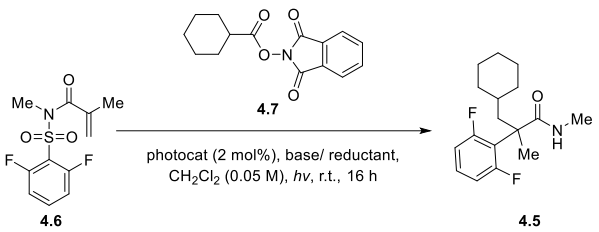

Entry	4.7 (equiv)	Reductant/ base	Catalyst	Light	Results
9	1.5	DIPEA (2.0 equiv)	/	dark	n.r.
10	/	/	$Ir(dtbbpy)ppy_2PF_6$	blue	n.r.
11	/	DIPEA (2.0 equiv)	$Ir(dtbbpy)ppy_2PF_6$	blue	n.r.

S.m. = starting material, n.r. = no reaction.

Inefficient decarboxylation of **4.7** was unlikely as its photocatalysed decarboxylation followed by addition to a Michael acceptor was well precedented. We attempted the study on two model substrates **4.8** and **4.9**. Despite the incomplete consumption of **4.9**, as predicted, the alkyl radical generated from **4.8** was successfully added to **4.9**, as shown in the crude ^{1}H NMR spectrum *(Scheme 50)*.

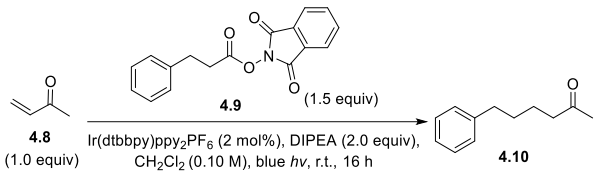

*Scheme 50 Decarboxylative alkyl coupling of N-hydroxyphthalimide ester **4.9** to **4.8***

Since it might be possible for the amide nitrogen in **4.6** to interact with the photoredox cycle, a different strategy was attempted. Hantzsch esters have been shown to form EDA complexes with the *N*-hydroxyphthalimide esters. Under purple light, the N-O bond is reduced, triggering subsequent alkyl decarboxylation and radical generation.[74] We attempted to use this Hantzsch ester system in various solvents, but all starting material was degraded. We proposed the less reactive sulfonyl methacrylamide substrates could be used in future investigations.

Table 14 Solvent screen for HE as reductant

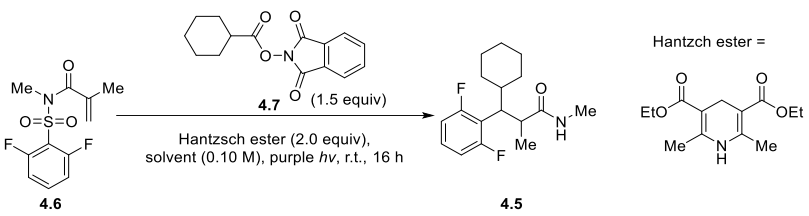

Entry	Solvent	Result
12	MeCN	s.m. degraded
13	DMA	s.m. degraded
14	THF	s.m. degraded

S.m. = starting material.

Chapter 5 Conclusion

Various radical Truce-Smiles reactions have been investigated using photoredox catalysis. In the first half of this work, we attempted to combine the mild photocatalysed aryl decarboxylative generation of aryl radicals with the radical Smiles rearrangement on aryl sulfonamides and sulfonates. We identified the pyridine-class of base as being effective for aryl decarboxylation in one of the aryl sulfonamide substrates, successfully deprotonating the carboxylic acid, leading to aryl decarboxylation. However, it was still challenging to find a proper base that is both effective in promoting decarboxylation whilst not being a potential coupling partner of the aryl radical.

In the second half of this work, tandem radical Smiles reactions were studied intra- and intermolecularly using two different methods of primary alkyl radical generation. A Michael-acceptor was incorporated to form a secondary radical for the Smiles rearrangement. We attempted to extend the idea of strain-release generated alkyl radicals initiated Truce-Smiles rearrangement[65] developed by our group by adding a Michael-acceptor to the system to study the intramolecular tandem Smiles reaction. In the proposed oxidative quenching catalytic cycle, reductants were critical in regenerating the photocatalyst. From our experiments, weak reductants were not able to induce N-O fission, while stronger reductants were incompatible with the Michael-acceptor and led to substrate degradation.

In an attempt to overcome substrate instability, the tandem process was investigated intermolecularly by having the primary radical generation site separate from the substrate, thus an alkyl *N*-hydroxyphthalimide ester was used as an external alkyl radical source. Although trace amounts of the Smiles product were observed in the multiple oxidative catalytic systems attempted, most of the starting material was degraded due to undesired interactions between the *N*-alkyl sulfonyl methacrylamide substrate and the alkyl decarboxylation catalytic cycle, despite being under mild conditions. A similar degradation pattern was observed in an alternative approach where a Hantzch ester was proposed to reduce *N*-hydroxyphthalimide ester upon visible light activation. These results suggested that the *N*-alkyl sulfonyl

methacrylamide substrate was too reactive in these photoredox conditions. As suggested by the literature, the *N*-side chain may affect the nucleophilicity on the nitrogen leading to different reactivites on the sulfonyl methacrylamide.[35c] To find a less reactive substrate to study the current tandem Smiles reaction, adjustments could be made on the *N*-side chain.

Substrates **4.11** and **4.12** with a different substituent at the nitrogen are proposed for further investigation *(Scheme 51)*. We suggest that replacing the alkyl substituent with phenyl or benzyl may modify the electronic properties at the nitrogen and reduce possible side reactions. Apart from the secondary alkyl radical, primary or tertiary radicals generated from the alkyl *N*-hydroxylphthlimide are also worth future exploration as they might reveal different reactivity towards the alkene in sulfonyl methacrylamides.

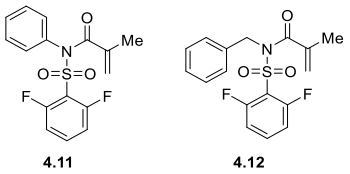

4.11 **4.12**

*Scheme 51 Proposed sulfonyl methacrylamide structures **4.11** and **4.12***

In general, most of the photoreactions attempted were centered on the oxidative quenching cycle, while the crucial stoichiometric auxiliary in turning over the catalytic cycle was interacting with the sulfonamide substrates in an undesired manner. Therefore, we believe developing redox neutral systems that are suitable for sulfonamide Smiles rearrangements will allow us to overcome the incompatibility issues experienced in these radical Smiles studies.

Chapter 6 Experimental Procedure and compound characterization

General Information

Stabilized, anhydrous solvents purchased from Millipore Sigma or Acro-Sealed were used in all photoreactions. All chemicals used were purchased from commercial suppliers (Sigma Aldrich, Alfa Aesar, Fisher Scientific, Fluka, Fluorochem) and used without further purification.

Thin layer chromatography (TLC) was performed on pre–coated Merck 60F254 silica plates that were visualized using a UV lamp (λ_{max} = 254 nm). Flash column chromatography was performed using the automatic Biotage Isolera machine with pore size 60 Å silica gel (350-400—mesh particle size) and Biotage KP-Sil or biotage Snap Ultra cartridges.

^{1}H-NMR, ^{13}C-NMR, ^{19}F-noCPD NMR spectra were recorded on a Bruker AVIII HD 400, Bruker AVIII 400, or Bruker AVIII HD 500 spectrometer with chemical shifts reported in ppm (parts per million) referenced to the residual solvent signal [^{1}H NMR: $CDCl_3$ (δ = 7.26), Acedone-d_6 (δ = 2.05), DMSO-d_6 (δ = 2.50), Acetonitrile-d_3 (δ = 1.94); ^{13}C NMR: $CDCl_3$ (δ = 77.16), Acetone-d_6 (δ = 29.84, 206.26), DMSO-d_6 (δ = 39.52), Acetonitrile-d_3 (δ = 1.32, 118.26)]. ^{19}F spectra were not calibrated to an internal standard. Coupling constants are reported to nearest 0.1Hz. The following abbreviations (or combinations thereof) are used in reporting multiplicities: br = broad, s = singlet, d = doublet, t = triplet, q = quartet, m = multiplet.

High-resolution mass (HRMS) spectra were obtained using a Waters QTOF with ESI/APCI ionisation and a Thermo Finnigan MAT95XP (EI).

Melting points in degrees Celsius were determined using a Kofler hot-stage apparatus or Stuart Scientific SMP10 apparatus and are uncorrected.

Purple light source Kessil PR160L-390 nm 40 W_{max}, tuneable blue and white light source Kessil A360W E-Series Tuna blue 90 W_{max}, and the green light source Warm Light Company green LED MR16 3 W were used in the photoreactions.

6.1.1 Synthesis of benzoic acid derivatives

A simple two-step synthesis was adapted to prepare sulfonylamido- or sulfonyloxy benzoic acid *(Scheme 52)*. Sulfonylamido and sulfonyloxy benzoate esters were synthesized following the modified general procedure A. Subsequently, the corresponding benzoic acids were obtained through base hydrolysis described in modified general procedure B.

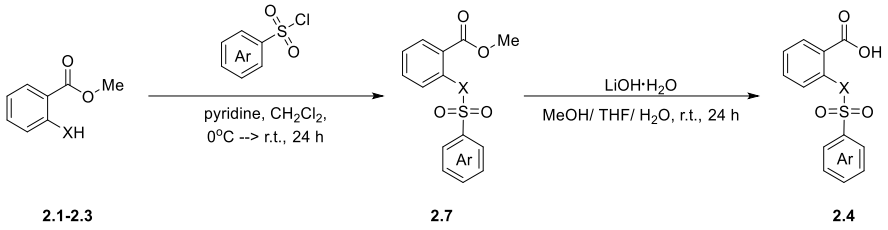

2.1-2.3 **2.7** **2.4**

Scheme 52 Synthesis of benzoic acid derivatives

General procedure A: *Synthesis of benzoate esters **2.7***

Following an adapted literature procedure[75], to a 100-mL round-bottom flask, pyridine (20 mmol, 4.0 equiv) was added dropwise to a solution of 2,6-difluorobenzene sulfonyl chloride (13 mmol, 2.6 equiv) and amino or hydroxy benzoate (5 mmol, 1.0 equiv) in dichloromethane (30 mL) at 0 °C. The reaction was warmed to room temperature and stirred for 24 hours. The reaction was quenched (30 mL) and washed with 1 M HCl (25 mL × 2). The organic layer was washed with brine (25 mL × 2), dried over anhydrous sodium sulfate, filtered, and collected. The organic portion was concentrated under reduced pressure and the crude product was purified by flash silica column chromatography.

Procedure B: *Hydrolysis of benzoate esters **2.4***

Reactions were conducted on a 300 mg scale. Following an adapted literature procedure, [76] to a 50-mL round-bottom flask, sulfonylamido or sulfonyloxy benzoate (1.0 equiv) was stirred with $LiOH{\cdot}H_2O$ (7.0 equiv) in 0.06 M THF/ MeOH/ H_2O (v/v/v; 5:3:2) at room temperature for 24 hours. Reactions were monitored by TLC. After consumption of the starting material, the reaction mixture was diluted with water (20 mL), then washed with ethyl acetate (20 mL × 3). The aqueous layer was collected and acidified to pH 2 with 2 M HCl. The benzoic acid was extracted with ethyl acetate (20

mL × 3). The combined organic layers were dried over anhydrous sodium sulfate and concentrated under reduced pressure to afford pure product.

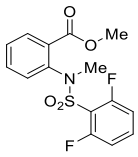

Methyl 2-[(2,6-difluoro-*N*-methylphenyl)sulfonamido]benzoate (2.7.1) was synthesized following procedure A using pyridine (1.6 mL, 20 mmol, 4.0 equiv), 2,6-difluorobenzene sulfonyl chloride (2.76 g, 13 mmol, 2.6 equiv), and dimethyl anthranilate (733 µL, 5 mmol, 1.0 equiv). The crude product was purified by flash silica column chromatography with (EA/ HEX; 15% → 30%) to afford the pure product as a shiny white powder (1.62 g, 95%).

^{1}H NMR (400 MHz, $CDCl_3$) δ 7.89 (dd, *J* = 7.6, 1.8 Hz, 1H), 7.48 (m, 2H), 7.41 (td, *J* = 7.6, 1.5 Hz, 1H), 7.19 (dd, *J* = 7.8, 1.4 Hz, 1H), 6.98 (m, 2H), 3.81 (s, 3H), 3.47 (s, 3H).
^{13}C NMR (126 MHz, $CDCl_3$) δ 166.43, 159.94 (dd, *J* = 259.5, 4.1 Hz), 139.48, 134.38 (t, *J* = 10.9 Hz), 132.94, 131.68, 131.53, 130.28, 128.90, 118.18 (t, *J* = 16.3 Hz), 113.14 (dd, *J* = 23.9, 3.8 Hz), 52.51, 39.86.
^{19}F NMR (376 MHz, $CDCl_3$) δ -104.96 (dd, *J* = 9.6, 5.8 Hz).
HR-ESI-MS (Acetone): 364.0418 ($[C_{15}H_{13}O_4NF_2NaS]^+$, ([M+Na]$^+$); calc. 364.0426, Δ = -2.08 ppm).
m.p. 70 – 72 °C (EA/ HEX).

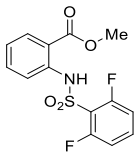

Methyl 2-[(2,6-difluorophenyl)sulfonamido]benzoate (2.7.2) was synthesized following procedure A using pyridine (1.6 mL, 20 mmol, 4.0 equiv), 2,6-difluorobenzene sulfonyl chloride (2.76 g, 13 mmol, 2.6 equiv), and methyl anthranilate (647 µL, 5 mmol, 1.0 equiv). The crude product was purified by flash silica column chromatography with (EA/ HEX; 15% → 30%) to yield the pure product as shiny white powder (1.64 g, *quant.*).

^{1}H NMR (400 MHz, $CDCl_3$) δ 11.17 (s, 1H), 7.92 (dd, *J* = 8.0, 1.6 Hz, 1H), 7.68 (dd, *J* = 8.3, 1.1 Hz, 1H), 7.39 (m, 2H), 6.99 (td, *J* = 8.1, 1.0 Hz, 1H), 6.90 (t, *J* = 8.9 Hz, 2H), 3.88 (s, 3H).

^{13}C NMR (101 MHz, $CDCl_3$) δ 168.35, 160.05 (dd, *J* = 259.9, 3.6 Hz), 139.87, 135.24 (t, *J* = 11.0 Hz), 134.89, 131.57, 123.10, 117.29, 117.12 (t, *J* = 15.3 Hz), 115.42, 113.24 (dd, *J* = 23.0, 3.8 Hz), 52.77.

^{19}F NMR (376 MHz, $CDCl_3$) δ -106.79 (dd, *J* = 8.8, 5.8 Hz).

HR-ESI-MS (Acetone): 350.0265 ($[C_{14}H_{11}O_4NF_2NaS]^+$, ($[M+Na]^+$); calc. 350.0269, Δ = -1.16 ppm).

m.p. 143 – 145 °C (EA/ HEX).

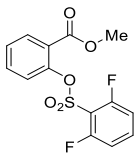

Methyl 2-{[(2,6-difluorophenyl)sulfonyl]oxy}benzoate (2.7.3) was synthesized following the modified literature procedure using pyridine (1.6 mL, 20 mmol, 4.0 equiv), 2,6-difluorobenzene sulfonyl chloride (2.76 g, 13 mmol, 2.6 equiv), and methyl salicylate (648 µL, 5 mmol, 1.0 equiv).[75b] The crude product was purified by flash silica column chromatography with (EA/ HEX; 10% → 20%) to yield the pure product as a white powder (1.62 g, 99%).

^{1}H NMR (400MHz, $CDCl_3$) δ 7.92 (dd, *J* = 7.8, 1.8 Hz, 1H), 7.64 (tt, *J* = 8.5, 5.8 Hz, 1H), 7.51 (dd, *J* = 7.4, 1.8 Hz, 1H), 7.37 (td, *J* = 7.6, 1.2 Hz, 1H), 7.20 (dd, *J* = 8.2, 1.2 Hz, 1H), 7.06 (t, *J* = 8.2 Hz, 2H), 3.81 (s, 3H).

^{13}C NMR (101 MHz, $CDCl_3$) δ 165.08, 160.11 (dd, *J* = 263.9, 3.1 Hz), 147.62, 136.66 (t, *J* = 11.0 Hz), 133.70, 132.40, 127.69, 125.28, 123.61, 114.49 (t, *J* = 15.4 Hz), 113.40 (dd, *J* = 23.3, 2.8 Hz), 52.56.

^{19}F NMR (376 MHz, $CDCl_3$) δ -103.91 (dd, *J* = 8.5, 5.8 Hz).

HR-ESI-MS (Acetone): 351.0103 ($[C_{14}H_{10}O_5F_2NaS]^+$, ($[M+Na]^+$); calc. 351.0109, Δ = -1.77 ppm).

m.p. 58 – 60 °C (EA/ HEX).

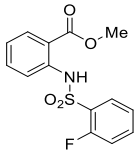

Methyl 2-[(2-fluoro-*N*-methylphenyl)sulfonamido]benzoate (2.7.4) was synthesized using pyridine (805µL, 10 mmol, 2.0 equiv), 2-fluorobenzene sulfonyl chloride (1.46 g, 7.5 mmol, 1.5 equiv), and methyl anthranilate (647 µL, 5.0 mmol, 1.0 equiv) following procedure A. The crude product was purified by flash silica column chromatography with (EA/ HEX; 10% → 25%) to yield the pure product as pink powder (1.55 g, *quant.*).

^{1}H NMR (400 MHz, $CDCl_3$) δ 11.02 (s, 1H), 7.97 (ddd, *J* = 15.3, 7.7, 1.7 Hz, 2H), 7.62 (dd, *J* = 8.4, 1.1 Hz, 1H), 7.58 – 7.48 (m, 1H), 7.40 (ddd, *J* = 8.7, 7.4, 1.7 Hz, 1H), 7.24 (td, *J* = 7.7, 1.6 Hz, 1H), 7.12 (ddd, *J* = 9.7, 8.3, 1.1 Hz, 1H), 7.02 (ddd, *J* = 8.2, 7.3, 1.1 Hz, 1H), 3.93 (s, 3H).

^{13}C NMR (101 MHz, $CDCl_3$) δ 168.30, 159.06 (d, *J* = 257.2 Hz), 140.03, 135.64 (d, *J* = 8.7 Hz), 134.61, 131.42, 131.06, 127.36 (d, *J* = 12.9 Hz), 124.43 (d, *J* = 3.9 Hz), 122.89, 117.91, 117.34 (d, *J* = 21.0 Hz), 115.69, 52.72.

^{19}F NMR (376 MHz, $CDCl_3$) δ -109.18 (ddd, *J* = 10.0, 7.2, 4.9 Hz).

HR-ESI-MS (Acetone): 332.0356 ($[C_{14}H_{12}O_4NFNaS]^+$, ($[M+Na]^+$); calc. 332.0363, Δ = -2.19 ppm).

m.p. 138 – 139 °C (EA/ HEX).

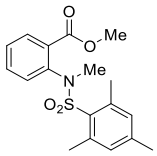

Methyl 2-[(*N*,2,4,6-tetramethylphenyl)sulfonamido]benzoate (2.7.5) was synthesized following a modified literature procedure[75a] using pyridine (805µL, 10 mmol, 2.0 equiv), mesityl sulfonyl chloride (2.19 g, 10.0 mmol, 2.0 equiv), and dimethyl anthranilate (733 µL, 5.0 mmol, 1.0 equiv) following procedure A. The crude product was purified by flash silica column chromatography with (EA/ HEX; 7% → 15%) to yield the pure product as a white powder (1.06 g, 61%).

^{1}H NMR (400 MHz, $CDCl_3$) δ 7.66 (dd, *J* = 7.7, 1.7 Hz, 1H), 7.46 (d, *J* = 7.3, 1.7 Hz, 1H), 7.36 (ddd, *J* = 14.8, 7.6, 1.3 Hz, 2H), 6.84 (s, 2H), 3.67 (s, 3H), 3.42 (s, 3H), 2.29 (s, 6H), 2.25 (s, 3H).

^{13}C NMR (101 MHz, $CDCl_3$) δ 166.52, 142.27, 140.21, 139.80, 133.28, 132.59, 132.50, 131.83, 131.62, 130.77, 128.41, 52.25, 39.82, 23.27, 21.03.

HR-ESI-MS (Acetone): 370.1077 ($[C_{18}H_{21}O_4NNaS]^+$, ([M+Na]$^+$); calc. 370.1084, Δ = -1.76 ppm).

m.p. 88 – 90 °C (EA/ HEX).

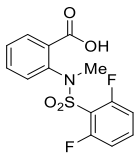

2-[(2,6-Difluoro-*N*-methylphenyl)sulfonamido]benzoic acid (2.4.1) was synthesized according to procedure B using **2.7.1** (300 mg, 0.88 mmol, 1.0 equiv) and $LiOH{\cdot}H_2O$ (258 mg, 6.15 mmol, 7.0 equiv). The crude product was purified by flash silica column chromatography with (CH_2Cl_2/ MeOH; 10% → 15%) to yield the pure product as a white powder (230 mg, 80%).

^{1}H NMR (400 MHz, DMSO-d_6) δ 13.01 (s, 1H), 7.81 (dd, *J* = 7.5, 1.9 Hz, 1H), 7.75 (tt, *J* = 8.4, 6.0 Hz, 1H), 7.50 (dtd, *J* = 20.3, 7.4, 1.6 Hz, 2H), 7.28 (t, *J* = 9.0 Hz, 2H), 7.14 (dd, *J* = 7.7, 1.5 Hz, 1H), 3.34 (s, 3H).

^{13}C NMR (101 MHz, DMSO-d_6) δ 167.36, 159.30 (dd, *J* = 256.9, 4.1 Hz), 139.00, 136.28 (t, *J* = 11.2 Hz), 132.98, 132.94, 131.26, 129.82, 129.26, 117.02 (t, *J* = 16.7 Hz), 114.00 (dd, *J* = 23.8, 3.5 Hz), 57.17.

^{19}F NMR (376 MHz, DMSO-d_6) δ -106.09 (dd, *J* = 10.6, 6.4 Hz)

HR-ESI-MS (Acetone): 350.0264 ($[C_{14}H_1O_4NF_2NaS]^+$, ([M+Na]$^+$); calc. 350.0269, Δ = -1.45 ppm).

m.p. 162 – 164 °C (EA/ HEX).

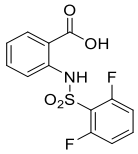

2-[(2,6-Difluorophenyl)sulfonamido]benzoic acid (2.4.2) was synthesized following procedure B using **2.7.2** (300 mg, 0.92 mmol, 1.0 equiv) and $LiOH{\cdot}H_2O$ (269 mg, 6.42 mmol, 7.0 equiv). Pure product was obtained as white solid (288 mg, *quant.*).

^{1}H NMR (400 MHz, DMSO-d_6) δ 11.70 (s, br, 1H), 7.96 (dd, *J* = 7.9, 1.6 Hz, 1H), 7.73 (tt, *J* = 8.5, 6.1 Hz, 1H), 7.56 (dtd, *J* = 16.9, 8.5, 1.5 Hz, 2H), 7.29 (t, *J* = 9.1 Hz, 2H), 7.16 (ddd, *J* = 8.2, 7.1, 1.4 Hz, 1H).

^{13}C NMR (101 MHz, DMSO-d_6) δ 169.75, 158.99 (dd, *J* = 257.5, 3.6 Hz), 139.01, 136.87 (t, *J* = 11.3 Hz), 134.77, 131.81, 123.76, 117.09, 116.50, 115.66 (t, *J* = 15.6 Hz), 113.69 (dd, *J* = 22.9, 3.4 Hz).

^{19}F NMR (376 MHz, DMSO-d_6) δ -108.29 (dd, *J* = 10.1, 6.3 Hz).

HR-ESI-MS (Acetone): 312.0137 ($[C_{13}H_8O_4NF_2S]^-$, ($[M-H]^-$); calc. 312.0148, Δ = -3.39 ppm).

m.p. 200 – 202 °C (EA/ HEX).

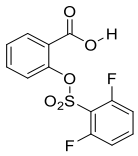

2-{[(2,6-Difluorophenyl)sulfonyl]oxy}benzoic acid (2.4.3) was synthesized following procedure B using **2.7.3** (300 mg, 0.91 mmol, 1.0 equiv) and $LiOH{\cdot}H_2O$ (268 mg, 6.40 mmol, 7.0 equiv). Pure product was obtained as white solid (214 mg, 75%).

^{1}H NMR (400 MHz, DMSO-d_6) δ 13.3 (s, 1H), 7.89 (m, 2H), 7.61 (td, *J* = 7.7, 1.8 Hz, 1H), 7.48 (td, *J* = 7.7, 1.2 Hz, 1H), 7.39 (t, *J* = 11.8 Hz, 2H), 7.13 (d, *J* = 8.2 Hz, 1H).

^{13}C NMR (101 MHz, DMSO-d_6) δ 165.19, 159.06 (dd, *J* = 260.7, 3.0 Hz), 146.83, 138.35 (t, *J* = 11.4 Hz), 133.70, 131.85, 128.08, 126.11, 123.24, 113.92 (dd, *J* = 23.3, 2.6 Hz), 112.90 (t, *J* = 15.3 Hz).

^{19}F NMR (376 MHz, DMSO-d_6) δ -105.82 (dd, *J* = 9.2, 6.1 Hz).

HR-ESI-MS (Acetone): 336.9948 ($[C_{13}H_8O_5F_2NaS]^+$, ($[M+Na]^+$); calc. 336.9953, Δ = -1.38 ppm).

m.p. 138 – 140 °C.

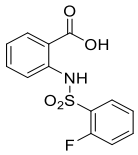

2-[(2-Fluorophenyl)sulfonamido]benzoic acid (2.4.4) was synthesized following procedure B using **2.7.4** (300 mg, 0.97 mmol, 1.0 equiv) and $LiOH \cdot H_2O$ (285 mg, 6.79 mmol, 7.0 equiv). Pure product was obtained as white solid (286 mg, *quant.*).

^{1}H NMR (400 MHz, DMSO-d_6) δ 11.51 (s, 1H), 7.95 (dd, *J* = 14.6, 7.8 Hz, 2H), 7.72 (dd, *J* = 5.8, 2.2 Hz, 1H), 7.56 – 7.36 (m, 4H), 7.12 (t, *J* = 6.8 Hz, 1H).

^{13}C NMR (101 MHz, DMSO-d_6) δ 169.79, 158.03 (d, *J* = 254.5 Hz), 139.26, 136.76 (d, *J* = 8.6 Hz), 134.63, 131.67, 130.81, 125.94 (d, *J* = 13.5 Hz), 125.22 (d, *J* = 3.8 Hz), 123.40, 117.49 (d, *J* = 19.3 Hz), 117.39, 116.33.

^{19}F NMR (376 MHz, DMSO-d_6) δ -110.91 (ddd, *J* = 10.8, 7.3, 5.4 Hz).

HR-ESI-MS (Acetone): 318.0204 ($[C_{13}H_{10}O_4NFNaS]^+$, ($[M+Na]^+$); calc. 318.0207, Δ = -0.87 ppm).

m.p. 196 – 198 °C (EA/ HEX).

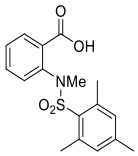

2-[(*N*,2,4,6-Tetramethylphenyl)sulfonamido]benzoic acid (2.4.5) was synthesized following procedure B using **2.7.5** (300 mg, 0.86 mmol, 1.0 equiv) and $LiOH \cdot H_2O$ (254 mg, 6.04 mmol, 7.0 equiv). Pure product was obtained as white solid (201 mg, 70%).

^{1}H NMR (400 MHz, DMSO-d_6) δ 12.82 (s, 1H), 7.67 (d, *J* = 7.6 Hz, 1H), 7.49 (ddd, *J* = 7.7, 4.7, 1.8 Hz, 1H), 7.43 (ddd, *J* = 7.7, 4.8, 1.8 Hz, 1H), 7.20 (d, *J* = 7.9 Hz, 1H), 6.96 (s, 2H), 3.28 (s, 3H), 2.23 (s, 9H).

^{13}C NMR (101 MHz, DMSO- d_6) δ 167.33, 142.27, 139.52, 139.05, 133.67, 133.04, 132.20, 131.93, 130.75, 130.52, 128.63, 39.52, 22.90, 20.63.

HR-ESI-MS (Acetone): 356.0925 ($[C_{17}H_{19}O_4NNaS]^+$, ([M+Na]$^+$); calc. 356.0927, Δ = -0.56 ppm).

m.p. 184 – 186 °C (EA/ HEX).

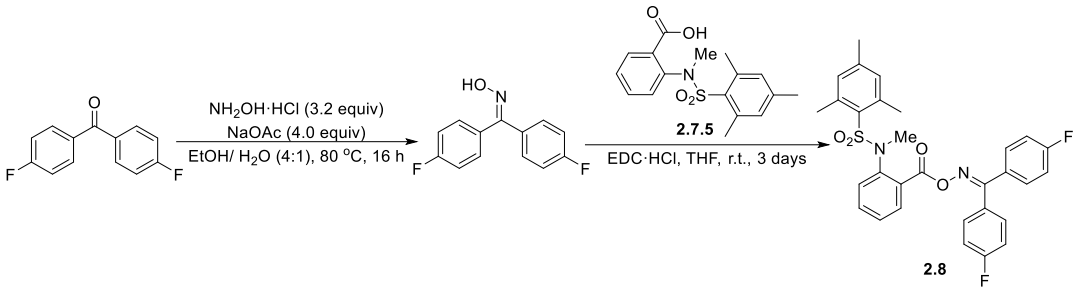

*Scheme 53 Synthesis of oxime ester **2.8***

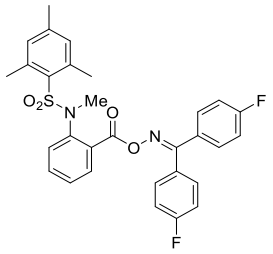

***N*-{2-[({[Bis(4-fluorophenyl)methylene]amino}oxy)carbonyl]phenyl}-*N*,2,4,6-tetramethylbenzenesulfonamide (2.8)** was synthesized following modified literature procedures.[77] To a 50 mL round-bottom flask, hydroxyamine hydrochloride (1.25 g, 18 mmol, 1.8 equiv) and sodium acetate (1.80 g, 22 mmol, 2.2 equiv) were added to a solution of bis(4-fluorophenyl)methanone (2.18 g, 10 mmol, 1.0 equiv) in 25 mL EtOH/ H_2O (4:1; v/v). The reaction was heated to reflux at 80 °C in air. The reaction was monitored by TLC and upon completion, the reaction mixture was cooled to room temperature, diluted with water (30 mL) and extracted with ethyl acetate (20 mL × 3). The combined organic layers were dried over anhydrous sodium sulfate and concentrated in *vacuo*. The crude bis(4-fluorophenyl)methanone oxime residue was obtained as a white solid and used in further synthesis without further purification.

To a solution of bis(4-fluorophenyl)methanone oxime (81 mg, 0.348 mmol, 1.2 equiv) and 2-((*N*,2,4,6-tetramethylphenyl)sulfonamido)benzoic acid **2.7.5** (100 mg, 0.29 mmol, 1.0 equiv) in dichloromethane (8 mL), 4-dimethylaminopyridine (4 mg, 0.029 mmol, 0.1 equiv) and EDC. HCl (278 mg, 1.45 mmol, 5.0 equiv) were added. The

reaction mixture was stirred at room temperature under nitrogen until completion (as shown by TLC). After reaction completion, the mixture was diluted with water (8 mL). The organic layer was collected, dried over anhydrous sodium sulfate, and concentrated under vacuo. The crude mixture was purified by flash column chromatography using (EA/ HEX; 30% → 50%) to yield pure product as white solid (56 mg, 35%).

^{1}H NMR (400 MHz, $CDCl_3$) δ 7.62 (dd, *J* = 8.9, 5.4 Hz, 2H), 7.45 (dt, *J* = 7.2, 1.7 Hz, 2H), 7.35 – 7.28 (m, 4H), 7.18 – 7.05 (m, 4H), 6.84 (s, 2H), 3.15 (s, 3H), 2.30 (s, 6H), 2.22 (s, 3H).

^{13}C NMR (101 MHz, $CDCl_3$) δ 164.76 (d, *J* = 252.5 Hz), 163.42 (d, *J* = 251.3 Hz), 163.28, 163.02, 142.46, 140.41, 140.37, 132.80, 132.68, 131.97, 131.38 (d, *J* = 6.0 Hz), 131.30 (d, *J* = 6.3 Hz), 131.15, 131.04, 130.94 (d, *J* = 3.3 Hz), 130.74, 128.48 (d, *J* = 3.7 Hz), 128.39, 115.87 (d, *J* = 17.1 Hz), 115.65 (d, *J* = 16.8 Hz), 39.49, 23.29, 21.21.

^{19}F NMR (376 MHz, $CDCl_3$) δ -108.62 (tt, *J* = 8.3, 5.4 Hz), -109.80 (tt, *J* = 8.4, 5.4 Hz).

HR-ESI-MS (Acetone): 571.1475 ($[C_{30}H_{26}O_4N_2F_2NaS]^+$, ($[M+Na]^+$); calc. 571.1474, Δ = 0.25 ppm).

m.p. 148 – 150 °C (EA/ HEX).

6.1.2 General Procedure for Photoreactions

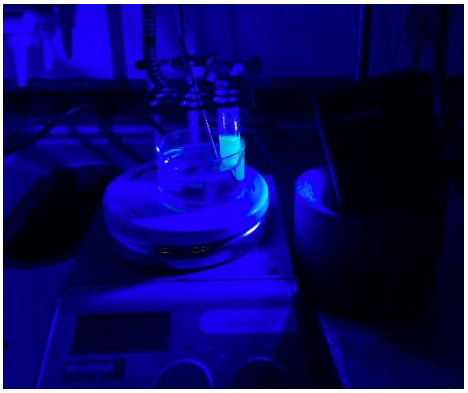

Figure 1 Photoreaction set up

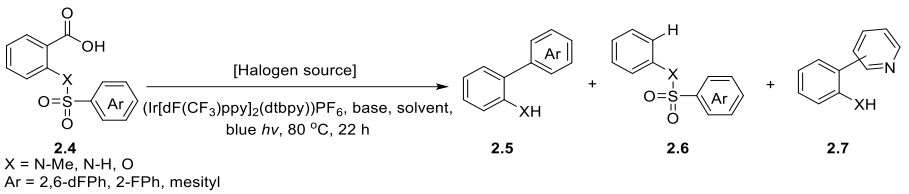

Scheme 54 Visible-light mediated aryl decarboxylative coupling of benzoic acid derivatives

To an oven-dried 8 mL microwave vial equipped with stirrer bar, all solid reagents were added and capped. The vial was evacuated and refilled with nitrogen three times. Anhydrous solvent, base (liquid), and halogen source (liquid) were added under nitrogen. The reaction mixture was bubbled with nitrogen for ten minutes. The reaction vial was placed 5 cm away from the blue light source and stirred at the stated temperature in an oil bath. The reaction was cooled to room temperature after 22 hours. The solvent was removed under reduced pressure. The residue was redissolved in deuterated solvent for NMR spectroscopic measurement of the crude.

6.2.1 Synthesis of cyclobutaneoxime ester

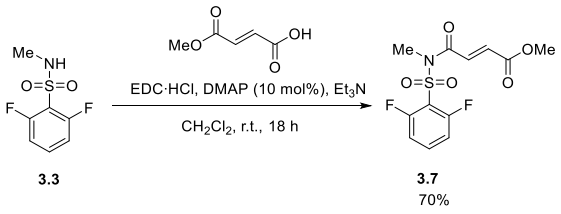

*Scheme 55 Synthesis of **3.7***

Methyl (*E*)-4-[(2,6-difluoro-*N*-methylphenyl)sulfonamido]-4-oxobut-2-enoate (3.7) was synthesized following a modified literature procedure.[33] To a suspension of **3.3** (300 mg, 1.45 mmol, 1.0 equiv), EDC·HCl (1.09 g, 5.68 mmol, 4.0 equiv), triethylamine (1.0 mL, 7.25 mmol, 5.0 equiv) and DMAP (18 mg, 0.15 mmol, 0.1 equiv) in dichloromethane (10 mL), mono-methyl fumarate (174 µL, 1.74 mmol, 1.2 equiv) was added at 0 °C. The reaction was stirred overnight at room temperature and monitored by TLC. After reaction completion, the resulting mixture was washed with 1N HCl (2 × 10mL), 1N $NaHCO_3$ (2 × 10mL), and water (1 × 10 mL). The organic layer was dried over anhydrous sodium sulfate and concentrated under reduced pressure to give a brown

residue. The crude product was purified by flash silica column chromatography with (EA/ HEX; 10% → 30%) to yield pure product as colourless oil (324 mg, 70%).

^{1}H NMR (400 MHz, $CDCl_3$) δ 7.65 (d, *J* = 15.3 Hz, 1H), 7.61 – 7.56 (m, 1H), 7.07 (t, *J* = 8.6 Hz, 2H), 6.76 (d, *J* = 15.3 Hz, 1H), 3.79 (s, 3H), 3.40 (s, 3H).
^{13}C NMR (101 MHz, $CDCl_3$) δ 165.22, 164.77, 159.78 (dd, *J* = 261.4, 3.2 Hz), 136.39 (t, *J* = 11.2 Hz), 134.49, 133.55, 117.08 (t, *J* = 15.1 Hz), 113.59 (dd, *J* = 23.4, 3.3 Hz), 52.54, 33.16.
^{19}F NMR (376 MHz, $CDCl_3$) δ -106.19 (dd, *J* = 9.2, 6.0 Hz).
HR-ESI-MS (Acetone): 342.0207 ($[C_{12}H_{11}O_5NF_2NaS]^+$, ($[M+Na]^+$); calc. 342.0218, Δ = -3.28 ppm).

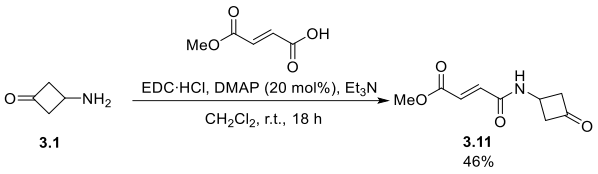

*Scheme 56 Synthesis of **3.11***

Methyl (*E*)-4-oxo-4-[(3-oxocyclobutyl)amino]but-2-enoate (3.11) was synthesized following a literature procedure.[33] To a solution of mono-methylfumarate (100 mg, 0.77 mmol, 1.0 equiv), 3-aminobutanone (187 mg, 1.54 mmol, 2.0 equiv), DMAP (188 mg, 0.15 mmol 0.2 equiv) and triethylamine (450 µL, 3.22 mmol, 4.2 equiv) in dichloromethane (2 mL), EDC·HCl (520 mg, 2.70 mmol, 3.5 equiv) was added. The reaction was stirred at room temperature under nitrogen for 18 hours. After completion, the reaction was diluted with dichloromethane (5 mL). The reaction mixture was washed with 1N $NaHCO_3$ (5mL × 1), water (5mL × 1), and brine (5mL × 1). The organic layer was dried over sodium sulfate and concentrated under reduced pressure to give a brownish-yellow solid. Crude product was purified by flash silica column chromatography with (EA/ HEX; 15% → 30%) to yield pure product as white solid (70 mg, 46%).

^{1}H NMR (400 MHz, $CDCl_3$) δ 7.38 (d, *J* = 5.8 Hz, 1H), 6.98 (d, *J* = 15.4 Hz, 1H), 6.83 (d, *J* = 15.5 Hz, 1H), 4.71 – 4.49 (m, 1H), 3.78 (s, 3H), 3.60 – 3.41 (m, 2H), 3.21 – 3.08 (m, 2H).
^{13}C NMR (101 MHz, $CDCl_3$) δ 204.92, 166.43, 163.98, 136.27, 130.42, 54.69, 52.56, 36.39.

HR-ESI-MS (Acetone): 220.0574 ([$C_9H_{11}O_4NNa]^+$, ([M+Na]$^+$); calc. 220.0580, Δ = -2.86 ppm).

m.p. 82 – 84 ^oC (EA/ HEX).

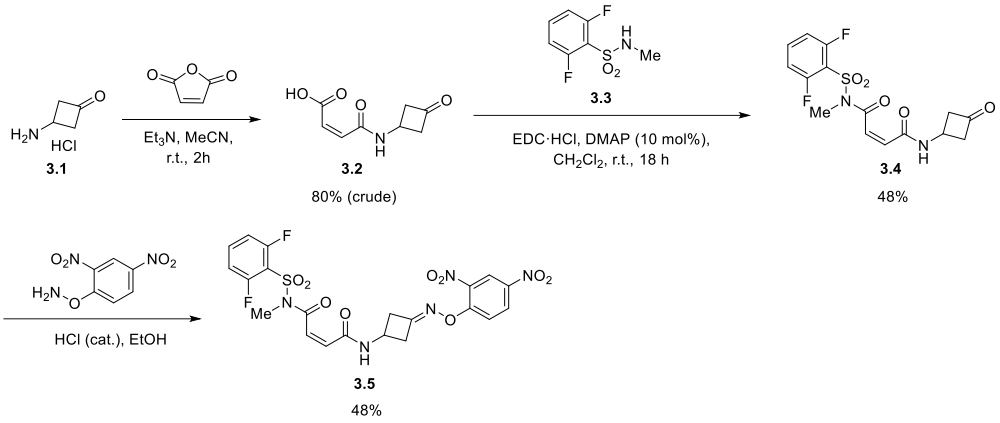

*Scheme 57 Synthetic scheme for cyclobutaneoxime ester **3.5***

3-Aminocyclobutan-1-one hydrochloride (**3.1)** was prepared following a literature procedure.[78] To a 50-mL round-bottom flask, *tert*-butyl (3-oxocyclobutyl) carbamate (1.30 g, 7 mmol) was suspended in dichloromethane (7 mL), then 4 N HCl (dioxane/ CH_2Cl_2) (7 mL) was added dropwise at 0 ^oC. The reaction was stirred overnight at room temperature. The solvent was removed under vacuo to afford a pale-yellow solid. The crude product was used for further synthesis without purification.

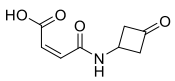

(*Z*)-4-Oxo-4-[(3-oxocyclobutyl)amino]but-2-enoic acid (3.2) was synthesized following a literature procedure.[79] To a 100-mL round-bottom flask, triethylamine (2.9 mL, 21.0 mmol, 7.0 equiv) was added dropwise to a solution of 3-aminocyclobutan-1-one hydrochloride (381 mg, 3.0 mmol, 1.0 equiv) and maleic anhydride (291 mg, 3.0 mmol, 1.0 equiv) in acetonitrile (20 mL). The reaction mixture was stirred at room temperature for 2 hours. The solvent was removed under reduced pressure. The minimum amount of water needed to dissolve the residue was added and concentrated HCl was added dropwise to the solution at 0 ^oC to adjust to pH to between 2 and 2.5. The solution was extracted with ethyl acetate (10 mL × 3). The

combined organic layers were dried over anhydrous sodium sulfate and concentrated under reduced pressure to give a pale-yellow solid. The crude product was used for further synthesis without purification.

2,6-Difluoro-*N*-methylbenzenesulfonamide (3.3) was prepared following a literature procedure.[80] To a 100-mL round-bottom flask, an aqueous solution of methylamine (40 wt%, 4 mL) was added dropwise to a solution of 2,6-difluorobenzenesulfonyl chloride (4.25 g, 20 mmol, 1.0 equiv) in diethyl ether (20 mL) at 0 °C. The reaction was warmed to room temperature and stirred further for 30 minutes. After reaction completion (as shown by TLC), the reaction mixture was allowed to rest for 5 minutes and two layers were observed. The upper organic layer was collected. The aqueous layer was extracted with ethyl acetate (10 mL × 3). The combined organic layers were washed with brine (10 mL × 1), dried over sodium sulfate and concentrated under vacuo to afford crude product as white solid. The crude product was used for further synthesis without purification.

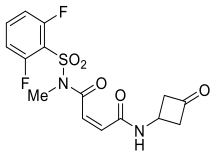

***N*^{1}-[(2,6-Difluorophenyl)sulfonyl]-*N*^{1}-methyl-*N*^{4}-(3-oxocyclobutyl)maleamide (3.4)** was synthesized following a literature procedure.[77] To an 8 mL microwave vial equipped with septum, EDC·HCl (207 mg, 1.2 mmol, 1.2 equiv) was added to the solution of (*Z*)-4-oxo-4-((3-oxocyclobutyl)amino)but-2-enoic acid **3.2** (183 mg, 1.0 mmol, 1.0 equiv), 2,6-difluoro-N-methylbenzenesulfonamide **3.3** (207 mg, 1.2 mmol, 1.2 equiv), and DMAP (12 mg, 0.1 mmol, 0.1 equiv) in dichloromethane (3 mL). The reaction was stirred at room temperature under nitrogen for 18 hours. After reaction completion, saturated $NaHCO_3$ solution (4 mL) was added to quench the reaction. The reaction was extracted with dichloromethane (5 mL × 3). The combined organic layers were dried over anhydrous sodium sulfate. The solvent was removed under reduced pressure to give a yellow oil. The crude product was purified by flash silica column

chromatography with (EA/ HEX; 10% → 50%) to yield pure product as white powder (178 mg, 48%).

^{1}H NMR (400 MHz, Acetone-d_6) δ 8.21 (s, 1H), 7.85 (tt, *J* = 8.5, 6.0 Hz, 1H), 7.55 (d, *J* = 14.9 Hz, 1H), 7.30 (t, *J* = 9.0 Hz, 2H), 6.93 (d, *J* = 14.9 Hz, 1H), 4.53 (dtd, *J* = 14.0, 7.9, 7.0, 4.1 Hz, 1H), 3.45 (s, 3H), 3.43 – 3.34 (m, 2H), 3.21 – 3.06 (m, 2H).
^{13}C NMR (101 MHz, Acetone-d_6) δ 204.70, 165.90, 163.79, 161.68 (d, *J* = 3.6 Hz), 159.11 (d, *J* = 3.4 Hz), 137.84, 130.31, 117.99 (t, *J* = 15.3, 13.4 Hz), 114.45 (dd, *J* = 23.3, 3.3 Hz), 54.65, 36.85, 33.41 (t, *J* = 2.4 Hz).
^{19}F NMR (376 MHz, Acetone-d_6) δ -108.43 (dd, *J* = 9.8, 6.0 Hz).
HR-ESI-MS (Acetone): 395.0475($[C_{15}H_{14}O_5N_2F_2NaS]^+$, ($[M+Na]^+$); calc. 395.0484, Δ = -2.20 ppm).
m.p. 164 – 166 °C (EA/ HEX).

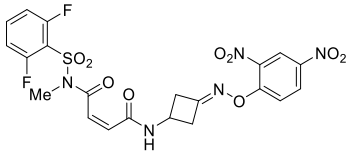

***N*^{1}-[(2,6-Difluorophenyl)sulfonyl]-*N*^{4}-{3-[(2,4-dinitrophenoxy)imino]cyclobutyl}-*N*^{1}-methylmaleamide (3.5)** was synthesized following a literature procedure.[60a] To a 10 mL vial, **3.4** (156 mg, 0.42 mmol, 1.0 equiv) and *o*-(2,4-dinitrophenyl)hydroxylamine (83 mg, 0.42 mmol, 1.0 equiv) were suspended in ethanol (4 mL, 0.1 M). Four drops of HCl were added slowly to the reaction mixture. The reaction was stirred at room temperature for 18 hours. Pure product was isolated by suction filtration as a white powder (112 mg, 48%).

^{1}H NMR (400 MHz, Acetone-d_6) δ 8.83 (d, *J* = 2.8 Hz, 1H), 8.55 (dd, *J* = 9.4, 2.8 Hz, 1H), 7.96 (d, *J* = 9.4 Hz, 1H), 7.92 – 7.80 (m, 1H), 7.57 (d, *J* = 14.9 Hz, 1H), 7.31 (t, *J* = 8.8 Hz, 2H), 6.92 (d, *J* = 15.0 Hz, 1H), 4.76 – 4.50 (m, 1H), 3.69 – 3.50 (m, 2H), 3.45 (s, 3H), 3.26 (ddddd, *J* = 15.7, 7.9, 6.3, 3.2, 1.4 Hz, 2H).
^{13}C NMR (126 MHz, Acetone- d_6) δ 165.87 (d, *J* = 3.3 Hz), 163.59, 163.51, 160.40 (dd, *J* = 258.9, 3.3 Hz), 157.75, 141.80, 137.90 (t, *J* = 11.3 Hz), 137.63, 137.59, 130.61, 130.36, 122.57, 117.96 (t, *J* = 15.8, 14.9 Hz), 117.89, 114.46 (dd, *J* = 22.3, 4.0 Hz), 40.25 (d, *J* = 6.8 Hz), 40.18 (d, *J* = 4.7 Hz), 39.93 (d, *J* = 3.4 Hz), 33.43 (t, *J* = 2.2 Hz).

^{19}F NMR (376 MHz, Acetone-d_6) δ -108.45 (dd, *J* = 9.8, 6.1 Hz).

HR-ESI-MS (Acetone): 576.0596 ($[C_{21}H_{17}O_9N_5F_2NaS]^+$, ($[M+Na]^+$); calc. 576.0607, Δ = -1.95 ppm).

m.p. 136 – 138 °C (decomp.) (EA/ HEX).

6.2.2 General Procedure of Photoreactions

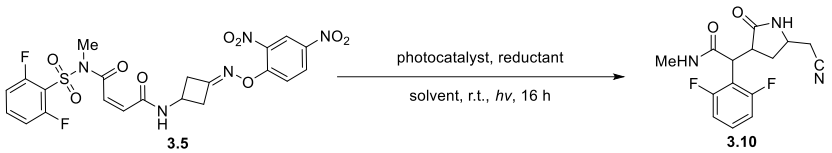

Scheme 58 Visible-light mediated strain-release cyclobutane ring-opening tandem Smiles reaction

To an oven-dried 8 mL microwave vial equipped with a stirrer bar, acrylamide **3.5** (0.1 mmol), photocatalyst, and reductant/ base (solid) were added and sealed. The vial was evacuated and refilled with nitrogen for three times. Anhydrous solvent and base (liquid) were added under nitrogen. The reaction mixture was bubbled with nitrogen for ten minutes. The reaction vial was placed at 5 cm away from the blue light source and stirred at room temperature for 16 hours. After reaction completion, the solvent was removed under reduced pressure. The residue was redissolved in deuterated solvent for crude NMR measurement.

6.3.1 Synthesis of sulfonylacrylamide and redox-active *N*-hydroxyphthalimide ester

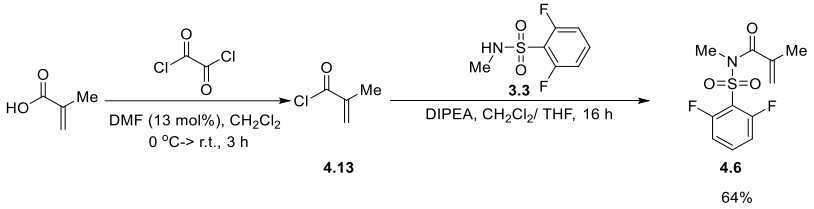

*Scheme 59 Synthesis of **4.6***

***N*-[(2,6-Difluorophenyl)sulfonyl]-*N*-methylmethacrylamide (4.6)** was synthesized following a modified literature procedures. [35b, 35c, 73]

To a microwave vial equipped with septum, oxalyl chloride (190 µL, 2.2 mmol, 2.2 equiv) was added dropwise to a solution of methacrylic acid (170 µL, 2.0 mmol, 2.0 equiv) in dichloromethane (2 mL). The reaction mixture was cooled to 0 °C, DMF (20 µL) was added dropwise under nitrogen. The reaction mixture was warmed to room temperature and stirred under nitrogen for 3 hours to give **4.13** as a yellow solution. The crude methacrylic chloride solution was used for further synthesis without purification.

To a microwave vial equipped with septum, sulfonamide **3.3** (207 mg, 1.0 mmol, 1.0 equiv) and DMAP (13 mg, 0.1 mmol, 0.1 equiv) were dissolved in (3 mL) CH_2Cl_2/ THF (1:1; v/v). The reaction mixture was cooled to 0 °C, DIPEA (350 µL, 2.0 mmol, 2.0 equiv), then methacrylic chloride solution **4.13** were added to the reaction mixture dropwise under nitrogen. The reaction mixture was warmed to room temperature and stirred under nitrogen for 16 hours. After reaction completion, the reaction was diluted with dichloromethane (10 mL) and quenched with sodium hydrogen carbonate solution (10 mL). The aqueous layer was extracted with dichloromethane (5 mL × 2). The combined organic layers were washed with brine (10 mL × 1), dried over anhydrous sodium sulfate and concentrated under reduced pressure to give a yellow oil. The crude product was purified by flash column chromatography using (EA/ HEX; 10% → 15%) to yield pure product as colourless oil (176 mg, 64%).

^{1}H NMR (400 MHz, $CDCl_3$) δ 7.68 – 7.47 (m, 1H), 7.04 (t, *J* = 8.6 Hz, 2H), 5.33 (d, *J* = 1.7 Hz, 1H), 5.13 (d, *J* = 1.3 Hz, 1H), 3.39 (s, 3H), 1.95 (s, 2H).
^{13}C NMR (101 MHz, $CDCl_3$) δ 172.38, 159.89 (dd, *J* = 260.7, 3.5 Hz), 140.08, 135.65 (t, *J* = 11.2 Hz), 119.94, 117.93 (t, *J* = 15.2 Hz), 113.29 (dd, *J* = 23.2, 3.6 Hz), 34.31, 19.48.
^{19}F NMR (376 MHz, $CDCl_3$) δ -106.56 (dd, *J* = 9.4, 6.0 Hz).
HR-ESI-MS (Acetone): 298.0312 ($[C_{11}H_{11}O_3NF_2NaS]^+$, ([M+Na]$^+$); calc. 298.0320, Δ = -2.66ppm).

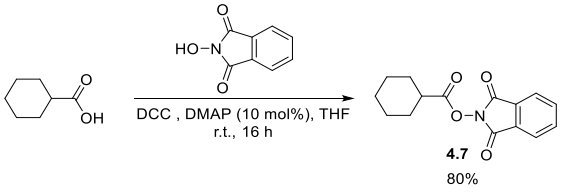

*Scheme 60 Synthesis of **4.7***

1,3-Dioxoisoindolin-2-yl cyclohexanecarboxylate (4.7) was prepared following a literature procedure. [17b, 17g] To a 100-mL round-bottom flask, cyclohexane carboxylic acid (385 mg, 3.0 mmol, 1.0 equiv), *N*-hydroxyphthalimide (538 mg, 3.3 mmol, 1.1 equiv), DMAP (37 mg, 0.3 mmol, 0.1 equiv), DCC (743 mg, 3.6 mmol, 1.2 equiv) were added to THF (15 mL) at 0 °C. The reaction was warmed to room temperature and stirred at room temperature under nitrogen for 16 h. The reaction was monitored by TLC. After reaction completion, the white solid was removed by suction filtration and the filtrate collected. The filtrate was concentrated under reduced pressure to give a colourless oil. The crude product was purified by flash silica column chromatography using (EA/ HEX; 5% → 15%) to yield pure product as a white powder (656 mg, 80%). Data is in accordance to literature.[17b, 17g]

^{1}H NMR (400 MHz, $CDCl_3$) δ 7.88 (dd, *J* = 5.5, 3.1 Hz, 2H), 7.78 (dd, *J* = 5.5, 3.1 Hz, 2H), 2.74 (tt, *J* = 10.9, 3.7 Hz, 1H), 2.18 – 2.05 (m, 2H), 1.92 – 1.79 (m, 2H), 1.75 – 1.60 (m, 3H), 1.45 – 1.24 (m, 3H).

^{13}C NMR (101 MHz, $CDCl_3$) δ 171.97, 162.25, 134.82, 129.18, 124.05, 40.63, 28.94, 25.62, 25.18.

HR-ESI-MS (Acetone): 296.0880 ($[C_{15}H_{15}O_4NNa]^+$, ($[M+Na]^+$); calc. 296.0893, Δ = -4.49 ppm).

m.p. 62 – 64 °C (EA/ HEX).

6.3.2 General Procedures for Photoreactions

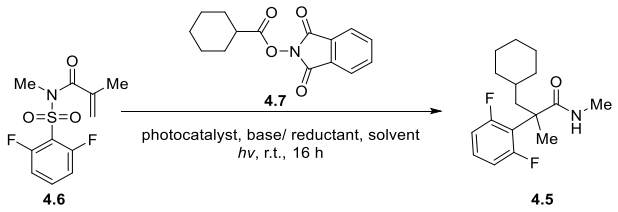

Scheme 61 Visible-light mediated alkyl decarboxylative tandem Smiles reaction

To an oven-dried microwave vial equipped with a stirrer bar, methacrylamide **4.6** (0.1 mmol), cyclohexyl *N*-hydroxyphthalimide ester **4.7**, photocatalyst, and reductant/ base (solid) were added and capped. The vial was evacuated and refilled with nitrogen three times. Freeze/pump/thaw procedure was performed three times in a microwave vial capped with anhydrous solvent. Solvent and base (liquid) were added to the reaction

under nitrogen. The reaction vial was placed at 5 cm away from the light source and stirred at room temperature for 16 h. Solvent was removed under reduced pressure. The residue was redissolved in deuterated solvent for NMR spectroscopic measurement of the crude.

Chapter 7 References

[1] M. Akita, T. Koike, *J. Synth. Org. Chem., Jpn.* **2016**, *74*, 1036-1046.

[2] J. K. McCusker, *Acc. Chem. Res.* **2003**, *36*, 876-887.

[3] C. K. Prier, D. A. Rankic, D. W. MacMillan, *Chem. Rev.* **2013**, *113*, 5322-5363.

[4] C. M. Holden, M. F. Greaney, *Chem. - Eur. J.* **2017**, *23*, 8992-9008.

[5] R. Henriques, *Ber. Dtsch. Chem. Ges.* **1894**, *27*, 2993-3005.

[6] (a) O. Hinsberg, *J. prakt. Chem.* **1914**, *90*, 345-353; (b) O. Hinsberg, *J. prakt. Chem.* **1916**, *93*, 277-301.

[7] (a) L. A. Warren, S. Smiles, *J. Chem. Soc.* **1930**, 1327-1331; (b) L. A. Warren, S. Smiles, *J. Chem. Soc.* **1930**, 956-963; (c) L. A. Warren, S. Smiles, *J. Chem. Soc.* **1932**, 2774-2778; (d) A. Levi, L. A. Warren, S. Smiles, *J. Chem. Soc.* **1933**, 1490-1493; (e) W. J. Evans, S. Smiles, *J. Chem. Soc.* **1935**, 181-188; (f) F. Galbraith, S. Smiles, *J. Chem. Soc.* **1935**, 1234-1238; (g) C. S. McClement, S. Smiles, *J. Chem. Soc.* **1937**, 1016-1021.

[8] W. E. Truce, E. M. Kreider, W. W. Brand, *Org. React.* **2004**, *18*, 99-215.

[9] (a) W. E. Truce, W. J. Ray Jr, *J. Am. Chem. Soc.* **1959**, *81*, 481-484; (b) W. E. Truce, W. J. Ray Jr, O. L. Norman, D. B. Eickemeyer, *J. Am. Chem. Soc.* **1958**, *80*, 3625-3629.

[10] (a) R. Loven, W. Speckamp, *Tetrahedron Lett.* **1972**, *13*, 1567-1570; (b) J. Köhler, W. Speckamp, *Tetrahedron Lett.* **1977**, *18*, 631-634.

[11] (a) W. B. Motherwell, A. M. Pennell, *J. Chem. Soc., Chem. Commun.* **1991**, 877-879; (b) M. L. E. da Mata, W. B. Motherwell, F. Ujjainwalla, *Tetrahedron Lett.* **1997**, *38*, 137-140; (c) M. L. E. da Mata, W. B. Motherwell, F. Ujjainwalla, *Tetrahedron Lett.* **1997**, *38*, 141-144.

[12] J. J. Douglas, H. Albright, M. J. Sevrin, K. P. Cole, C. R. Stephenson, *Angew. Chem., Int. Ed.* **2015**, *54*, 14898-14902.

[13] J. J. Douglas, M. J. Sevrin, K. P. Cole, C. R. Stephenson, *Org. Process Res. Dev.* **2016**, *20*, 1148-1155.

[14] P. Lan, C. J. Jackson, M. G. Banwell, A. C. Willis, *J. Org. Chem.* **2014**, *79*, 6759-6764.

[15] A. Sáenz-Galindo, L. I. López-López, N. Fabiola, A. O. Castañeda-Facio, L. A. Rámirez-Mendoza, K. C. Córdova-Cisneros, D. de Loera-Carrera, in *Carboxylic Acid: Key Roles in Life Sciences* (Eds.: G. L. Radu, G.-I. Badea), IntechOpen, London, **2018**, pp. 1-35.

[16] S. Karmakar, A. Silamkoti, N. A. Meanwell, A. Mathur, A. Gupta, *Adv. Synth. Catal.* **2021**.

[17] (a) K. Okada, K. Okamoto, N. Morita, K. Okubo, M. Oda, *J. Am. Chem. Soc.* **1991**, *113*, 9401-9402; (b) J. Schwarz, B. Koenig, *Green Chem.* **2016**, *18*, 4743-4749; (c) M. Jiang, Y. Jin, H. Yang, H. Fu, *Sci. Rep.* **2016**, *6*, 26161; (d) L. Ren, H. Cong, *Org. Lett.* **2018**, *20*, 3225-3228; (e) P. Ji, Y. Zhang, Y. Wei, H. Huang, W. Hu, P. A. Mariano, W. Wang, *Org. Lett.* **2019**, *21*, 3086-3092; (f) A. F. Garrido-Castro, H. Choubane, M. Daaou, M. C. Maestro, J. Aleman, *Chem. Commun. (Cambridge, U. K.)* **2017**, *53*, 7764-7767; (g) K. N. Tripathi, M. Belal, R. P. Singh, *J. Org. Chem.* **2019**, *85*, 1193-1201; (h) G. L. Dai, S. Z. Lai, Z. Luo, Z. Y. Tang, *Org. Lett.* **2019**, *21*, 2269-2272; (i) J. Schwarz, B. König, *ChemPhotoChem* **2017**, *1*, 237-242; (j) J. Yang, J. Zhang, L. Qi, C. Hu, Y. Chen, *Chem. Commun.* **2015**, *51*, 5275-5278; (k) I. S. Wan, M. D. Witte, A. J. Minnaard, *Org. Lett.* **2019**, *21*, 7669-7673.

[18] H. Meerwein, E. Büchner, K. van Emster, *J. prakt. Chem.* **1939**, *152*, 237-266.

[19] (a) F. W. Friese, C. Mück-Lichtenfeld, A. Studer, *Nat. Commun.* **2018**, *9*, 1-7; (b) K. A. Hollister, E. S. Conner, M. L. Spell, K. Deveaux, L. Maneval, M. W. Beal, J. R. Ragains, *Angew. Chem.* **2015**, *127*, 7948-7952; (c) A.-F. Voica, A. Mendoza, W. R. Gutekunst, J. O. Fraga, P. S. Baran, *Nat. Chem.* **2012**, *4*, 629-635; (d) M. Heinrich, A. Gansäuer*, Vol. 320*, Springer Science & Business Media, Berlin, **2012**, pp. 33-59.

[20] N. Kvasovs, V. Gevorgyan, *Chem. Soc. Rev.* **2021**, *50*, 2244-2259.

[21] J. Chateauneuf, J. Lusztyk, K. U. Ingold, *J. Am. Chem. Soc.* **1988**, *110*, 2886-2893.
[22] S. Seo, J. B. Taylor, M. F. Greaney, *Chem. Commun.* **2012**, *48*, 8270-8272.
[23] L. Candish, M. Teders, F. Glorius, *J. Am. Chem. Soc.* **2017**, *139*, 7440-7443.
[24] T. Patra, S. Mukherjee, J. Ma, F. Strieth-Kalthoff, F. Glorius, *Angew. Chem.* **2019**, *131*, 10624-10630.
[25] (a) P. Xu, P. López-Rojas, T. Ritter, *J. Am. Chem. Soc.* **2021**, *143*, 5349-5354; (b) T. Q. Chen, P. S. Pedersen, N. W. Dow, R. Fayad, C. E. Hauke, M. C. Rosko, E. O. Danilov, D. C. Blakemore, A.-M. Dechert-Schmitt, T. Knauber, *ChemRxiv* **2021**.
[26] L. Candish, M. Freitag, T. Gensch, F. Glorius, *Chem. Sci.* **2017**, *8*, 3618-3622.
[27] (a) S. Ni, Y. Zhang, C. Xie, H. Mei, J. Han, Y. Pan, *Org. Lett.* **2015**, *17*, 5524-5527; (b) G. Zheng, Y. Li, J. Han, T. Xiong, Q. Zhang, *Nat. Commun.* **2015**, *6*, 1-9; (c) E. Brachet, L. Marzo, M. Selkti, B. Konig, P. Belmont, *Chem. Sci.* **2016**, *7*, 5002-5006; (d) D.-L. Kong, L. Cheng, H.-R. Wu, Y.-X. Li, D. Wang, L. Liu, *Org. Biomol. Chem.* **2016**, *14*, 2210-2217; (e) T. Miao, D. Xia, Y. Li, P. Li, L. Wang, *Chem. Commun. (Cambridge, U. K.)* **2016**, *52*, 3175-3178; (f) C. Pan, H. Zhang, C. Zhu, *Tetrahedron Lett.* **2016**, *57*, 595-598; (g) Z.-S. Wang, Y.-B. Chen, H.-W. Zhang, Z. Sun, C. Zhu, L.-W. Ye, *J. Am. Chem. Soc.* **2020**, *142*, 3636-3644; (h) J. Yan, H. W. Cheo, W. K. Teo, X. Shi, H. Wu, S. B. Idres, L.-W. Deng, J. Wu, *J. Am. Chem. Soc.* **2020**, *142*, 11357-11362.
[28] F. Ujjainwalla, M. L. E. da Mata, A. M. Pennell, C. Escolano, W. B. Motherwell, S. Vazquez, *Tetrahedron* **2015**, *71*, 6701-6719.
[29] H. Chen, L. Wang, J. Han, *Chem. Commun.* **2020**, *56*, 5697-5700.
[30] E. D. Nacsa, T. H. Lambert, *Org. Chem. Front.* **2018**, *5*, 64-69.
[31] (a) V. G. Haensch, T. Neuwirth, J. Steinmetzer, F. Kloss, R. Beckert, S. Grafe, S. Kupfer, C. Hertweck, *Chem. - Eur. J.* **2019**, *25*, 16068; (b) F. Kloss, T. Neuwirth, V. G. Haensch, C. Hertweck, *Angew. Chem., Int. Ed.* **2018**, *57*, 14476-14481.
[32] G. Revol, T. McCallum, M. Morin, F. Gagosz, L. Barriault, *Angew. Chem., Int. Ed.* **2013**, *52*, 13342-13345.
[33] M. Pudlo, I. Allart-Simon, B. Tinant, S. Gerard, J. Sapi, *Chem. Commun.* **2012**, *48*, 2442-2444.
[34] J.-L. Tu, W. Tang, F. Liu, *Org. Chem. Front.* **2021**, *8*, 3712-3717.
[35] (a) N. Fuentes, W. Kong, L. Fernández-Sánchez, E. Merino, C. Nevado, *J. Am. Chem. Soc.* **2015**, *137*, 964-973; (b) W. Kong, M. Casimiro, N. Fuentes, E. Merino, C. Nevado, *Angew. Chem., Int. Ed.* **2013**, *52*, 13086-13090; (c) W. Kong, M. Casimiro, E. Merino, C. Nevado, *J. Am. Chem. Soc.* **2013**, *135*, 14480-14483; (d) W. Kong, N. Fuentes, A. García-Domínguez, E. Merino, C. Nevado, *Angew. Chem., Int. Ed.* **2015**, *54*, 2487-2491.
[36] C. Liu, B. Zhang, *RSC Adv.* **2015**, *5*, 61199-61203.
[37] Z. He, P. Tan, C. Ni, J. Hu, *Org. Lett.* **2015**, *17*, 1838-1841.
[38] B. Niu, P. Xie, Z. Bian, W. Zhao, M. Zhang, Y. Zhou, L. Feng, C. U. Pittman Jr, A. Zhou, *Synlett* **2015**, *26*, 635-638.
[39] Q. Tian, P. He, C. Kuang, *Org. Biomol. Chem.* **2014**, *12*, 6349-6353.
[40] Z. Ni, X. Huang, Y. Pan, *Org. Lett.* **2016**, *18*, 2612-2615.
[41] D. Whalley, H. Duong, M. Greaney, *Chem. - Eur. J.* **2019**, *25*, 1927-1930.
[42] D. M. Whalley, M. F. Greaney, *Nat. Chem.* **2021**, *13*, 304-305.
[43] C. Hervieu, M. S. Kirillova, T. Suarez, M. Muller, E. Merino, C. Nevado, *Nat. Chem.* **2021**, *13*, 327-334.
[44] C. Faderl, S. Budde, G. Kachkovskyi, D. Rackl, O. Reiser, *J. Org. Chem.* **2018**, *83*, 12192-12206.
[45] D. M. Whalley, H. A. Duong, M. F. Greaney, *Chem. Commun.* **2020**, *56*, 11493-11496.
[46] A. Hossian, R. Jana, *Org. Biomol. Chem.* **2016**, *14*, 9768-9779.
[47] J. C. Gonzalez-Gomez, N. P. Ramirez, T. Lana-Villarreal, P. Bonete, *Org. Biomol. Chem.* **2017**, *15*, 9680-9684.

[48] S. F. Wang, X. P. Cao, Y. Li, *Angew. Chem., Int. Ed.* **2017**, *56*, 13809-13813.
[49] A. R. Tripathy, G. S. Yedase, V. R. Yatham, *RSC Adv.* **2021**, *11*, 25207-25210.
[50] J. Boivin, A.-C. Callier-Dublanchet, B. Quiclet-Sire, A.-M. Schiano, S. Z. Zard, *Tetrahedron* **1995**, *51*, 6517-6528.
[51] T. Xiao, H. Huang, D. Anand, L. Zhou, *Synthesis* **2020**, *52*, 1585-1601.
[52] (a) F. F. Fleming, L. Yao, P. C. Ravikumar, L. Funk, B. C. Shook, *J. Med. Chem.* **2010**, *53*, 7902-7917; (b) H. Shirakawa, T. Masuda, K. Takeda, *The chemistry of triple-bonded functional groups, Vol. 2*, Wiley-Blackwell, **1994**; (c) T. Wang, N. Jiao, *Acc. Chem. Res.* **2014**, *47*, 1137-1145; (d) S. Patai, Z. Rappoport, in *The Chemistry of the Cyano Group* (Ed.: Z. Rappoport), Wiley, Jerusalem, **1970**, p. 307.
[53] J. Boivin, E. Fouquet, S. Z. Zard, *J. Am. Chem. Soc.* **1991**, *113*, 1055-1057.
[54] D. H. Barton, S. Z. Zard, *Pure Appl. Chem.* **1986**, *58*, 675-684.
[55] J. Boivin, A.-M. Schiano, S. Z. Zard, *Tetrahedron Lett.* **1992**, *33*, 7849-7852.
[56] H. B. Yang, N. Selander, *Chem. - Eur. J.* **2017**, *23*, 1779-1783.
[57] T. Nishimura, T. Yoshinaka, Y. Nishiguchi, Y. Maeda, S. Uemura, *Org. Lett.* **2005**, *7*, 2425-2427.
[58] B. Zhao, Z. Shi, *Angew. Chem.* **2017**, *129*, 12901-12905.
[59] Y. R. Gu, X. H. Duan, L. Yang, L. N. Guo, *Org. Lett.* **2017**, *19*, 5908-5911.
[60] (a) J. Davies, S. G. Booth, S. Essafi, R. A. Dryfe, D. Leonori, *Angew. Chem., Int. Ed.* **2015**, *54*, 14017-14021; (b) H. Jiang, X. An, K. Tong, T. Zheng, Y. Zhang, S. Yu, *Angew. Chem., Int. Ed.* **2015**, *54*, 4055-4059; (c) X. D. An, S. Yu, *Org. Lett.* **2015**, *17*, 2692-2695.
[61] J. Boivin, E. Fouquet, A.-M. Schiano, S. Z. Zard, *Tetrahedron* **1994**, *50*, 1769-1776.
[62] (a) E. M. Dauncey, S. P. Morcillo, J. J. Douglas, N. S. Sheikh, D. Leonori, *Angew. Chem., Int. Ed.* **2018**, *57*, 744-748; (b) J. Davies, N. S. Sheikh, D. Leonori, *Angew. Chem., Int. Ed.* **2017**, *56*, 13361-13365.
[63] H. Jiang, A. Studer, *Angew. Chem., Int. Ed.* **2017**, *56*, 12273-12276.
[64] (a) P.-Z. Wang, X.-Y. Yu, C.-Y. Li, B.-Q. He, J.-R. Chen, W.-J. Xiao, *Chem. Commun.* **2018**, *54*, 9925-9928; (b) S. Yao, K. Zhang, Q.-Q. Zhou, Y. Zhao, D.-Q. Shi, W.-J. Xiao, *Chem. Commun.* **2018**, *54*, 8096-8099; (c) X. Y. Yu, J. R. Chen, P. Z. Wang, M. N. Yang, D. Liang, W. J. Xiao, *Angew. Chem., Int. Ed.* **2018**, *57*, 738-743; (d) W. Zhang, Y.-L. Pan, C. Yang, X. Li, B. Wang, *Org. Chem. Front.* **2019**, *6*, 2765-2770; (e) L. Li, H. Chen, M. Mei, L. Zhou, *Chem. Commun. (Cambridge, U. K.)* **2017**, *53*, 11544-11547.
[65] D. M. Whalley, J. Seayad, M. F. Greaney, *Angew. Chem., Int. Ed.* **2021**, *60*, 22219-22223.
[66] W. O. Foye, R. K. Griffith, in *Foye's Principles of Medicinal Chemistry*, 6th ed. (Eds.: T. L. Lemke, D. A. Williams), Lippincott Williams & Wilkins, Philadelphia, **2008**, p. 414.
[67] (a) T. D. Claridge, *High-resolution NMR techniques in organic chemistry, Vol. 27*, Elsevier, **2016**; (b) H. Friebolin, J. K. Becconsall, *Basic one-and two-dimensional NMR spectroscopy, Vol. 7*, Wiley-vch Weinheim:, **2005**.
[68] (a) P. Lassalas, B. Gay, C. Lasfargeas, M. J. James, V. Tran, K. G. Vijayendran, K. R. Brunden, M. C. Kozlowski, C. J. Thomas, A. B. Smith, 3rd, D. M. Huryn, C. Ballatore, *J. Med. Chem.* **2016**, *59*, 3183-3203; (b) E. Noten, R. McAtee, C. Stephenson, *ChemRxiv* **2021**.
[69] (a) D. Avila, C. Brown, K. Ingold, J. Lusztyk, *J. Am. Chem. Soc.* **1993**, *115*, 466-470; (b) Y.-R. Luo, in *Handbook of bond dissociation energies in organic compounds*, CRC press, Boca Raton, **2002**, p. 76.
[70] (a) D. Basavaiah, G. Veeraraghavaiah, *Chem. Soc. Rev.* **2012**, *41*, 68-78; (b) D. Basavaiah, K. Venkateswara Rao, R. Jannapu Reddy, *Chem. Soc. Rev.* **2007**, *36*, 1581-1588; (c) E. Ciganek, *Org. React.* **2004**, *51*, 201-350; (d) D. Basavaiah, A. J. Rao, T. Satyanarayana, *Chem. Rev.* **2003**, *103*, 811-892; (e) D. Basavaiah, B. S. Reddy, S. S. Badsara, *Chem. Rev.* **2010**, *110*, 5447-5674.

[71] M. J. Sevrin, L. Furst, J. D. Nguyen, J. L. Collins III, C. R. Stephenson, *Tetrahedron* **2018**, *74*, 3246-3252.
[72] L. Buglioni, M. M. Mastandrea, A. Frontera, M. A. Pericas, *Chem. - Eur. J.* **2019**, *25*, 11785-11790.
[73] (a) H. Wang, S. Sun, J. Cheng, *Org. Lett.* **2017**, *19*, 5844-5847; (b) W. Kong, E. Merino, C. Nevado, *Angew. Chem., Int. Ed.* **2014**, *53*, 5078-5082.
[74] L. M. Kammer, S. O. Badir, R.-M. Hu, G. A. Molander, *Chem. Sci.* **2021**, *12*, 5450-5457.
[75] (a) A. Naganawa, T. Saito, Y. Nagao, H. Egashira, M. Iwahashi, T. Kambe, M. Koketsu, H. Yamamoto, M. Kobayashi, T. Maruyama, S. Ohuchida, H. Nakai, K. Kondo, M. Toda, *Bioorg. Med. Chem.* **2006**, *14*, 5562-5577; (b) J. Wang, J. Zhao, H. Gong, *Chem. Commun.* **2017**, *53*, 10180-10183.
[76] A. Jarvis, C. K. Allerston, H. Jia, B. Herzog, A. Garza-Garcia, N. Winfield, K. Ellard, R. Aqil, R. Lynch, C. Chapman, B. Hartzoulakis, J. Nally, M. Stewart, L. Cheng, M. Menon, M. Tickner, S. Djordjevic, P. C. Driscoll, I. Zachary, D. L. Selwood, *J. Med. Chem.* **2010**, *53*, 2215-2226.
[77] T. Patra, S. Mukherjee, J. Ma, F. Strieth-Kalthoff, F. Glorius, *Angew. Chem., Int. Ed.* **2019**, *58*, 10514-10520.
[78] W. Wang, L. Zhang, L. Morlock, N. S. Williams, J. W. Shay, J. K. De Brabander, *J. Med. Chem.* **2019**, *62*, 5217-5241.
[79] D. Moravčíková, A. Koreňová, D. Berkeš, in *A Synthesis of Conformationally Restricted Proline Chimeras, in Proceedings of the 16th International Electronic Conference on Synthetic Organic Chemistry*, **2012**.
[80] N. Ishida, Y. Shimamoto, M. Murakami, *Angew. Chem.* **2012**, *124*, 11920-11922.